AD-A174 334 MINORITY-CARRIER INVESTIGATIONS OF BEAM-ANNEALED AND THERMALLY-ANNEALED SEMICONDUCTORS(U) CALIFORNIA UNIV SANTA BARBARA J L MERZ SEP 86 RADC-TR-85-272 1/1

UNCLASSIFIED F19628-82-K-0006 F/G 20/12 NL

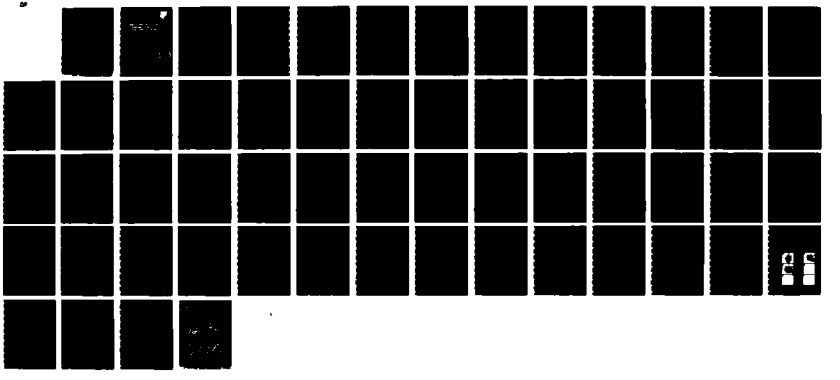

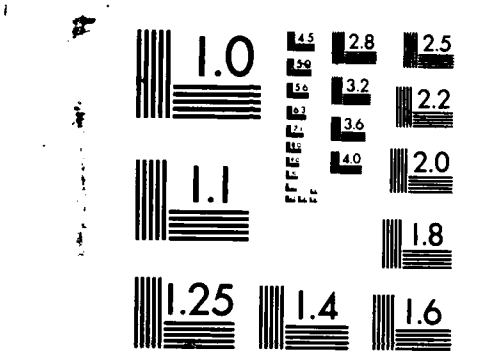

MICROCOPY RESOLUTION TEST CHART
NATIONAL BUREAU OF STANDARDS-1963-A

RADC-TR-85-272
Final Technical Report
September 1986

MINORITY-CARRIER INVESTIGATIONS OF BEAM-ANNEALED AND THERMALLY-ANNEALED SEMICONDUCTORS

University of California

James L. Merz

ROME AIR DEVELOPMENT CENTER
Air Force Systems Command
Griffiss Air Force Base, NY 13441-5700

This report has been reviewed by the RADC Public Affairs Office (PA) and is releasable to the National Technical Information Service (NTIS). At NTIS it will be releasable to the general public, including foreign nations.

RADC-TR-85-272 has been reviewed and is approved for publication.

APPROVED: Thomas G. Ryan

THOMAS G. RYAN
Project Engineer

APPROVED: Harold Roth

HAROLD ROTH, Director
Solid State Sciences Division

FOR THE COMMANDER: John A. Ritz

JOHN A. RITZ
Plans & Programs Division

If your address has changed or if you wish to be removed from the RADC mailing list, or if the addressee is no longer employed by your organization, please notify RADC (ESO) Hanscom AFB MA 01731-5000. This will assist us in maintaining a current mailing list.

Do not return copies of this report unless contractual obligations or notices on a specific document requires that it be returned.

REPORT DOCUMENTATION PAGE

1a. REPORT SECURITY CLASSIFICATION UNCLASSIFIED	1b. RESTRICTIVE MARKINGS N/A
2a. SECURITY CLASSIFICATION AUTHORITY N/A	3. DISTRIBUTION / AVAILABILITY OF REPORT Approved for public release; distribution unlimited.
2b. DECLASSIFICATION / DOWNGRADING SCHEDULE N/A	
4. PERFORMING ORGANIZATION REPORT NUMBER(S) N/A	5. MONITORING ORGANIZATION REPORT NUMBER(S) RADC-TR-85-272
6a. NAME OF PERFORMING ORGANIZATION University of California 6b. OFFICE SYMBOL (If applicable)	7a. NAME OF MONITORING ORGANIZATION Rome Air Development Center (ESO)
6c. ADDRESS (City, State, and ZIP Code) Santa Barbara CA 93106	7b. ADDRESS (City, State, and ZIP Code) Hanscom AFB MA 01731-5000
8a. NAME OF FUNDING / SPONSORING ORGANIZATION Rome Air Development Center 8b. OFFICE SYMBOL (If applicable) ESO	9. PROCUREMENT INSTRUMENT IDENTIFICATION NUMBER F19628-82-K-0006
8c. ADDRESS (City, State, and ZIP Code) Hanscom AFB MA 01731-5000	10. SOURCE OF FUNDING NUMBERS PROGRAM ELEMENT NO. 61102F; PROJECT NO. 2306; TASK NO. J2; WORK UNIT ACCESSION NO. 43

11. TITLE (Include Security Classification)
MINORITY-CARRIER INVESTIGATIONS OF BEAM-ANNEALED AND THERMALLY-ANNEALED SEMICONDUCTORS

12. PERSONAL AUTHOR(S)
James L. Merz

13a. TYPE OF REPORT	13b. TIME COVERED	14. DATE OF REPORT (Year, Month, Day)	15. PAGE COUNT
Final	FROM Oct 81 TO Oct 85	September 1986	60

16. SUPPLEMENTARY NOTATION
N/A

17. COSATI CODES		
FIELD	GROUP	SUB-GROUP
09	01	

18. SUBJECT TERMS (Continue on reverse if necessary and identify by block number)
Minority-Carrier, Thermally-Annealed, Beam-Annealed, Semiconductor

19. ABSTRACT (Continue on reverse if necessary and identify by block number)

The effect of beam-processing on III-V compound semiconductors, particularly indium phosphide (InP), has been investigated in detail. Two types of "beams" have been used to anneal ion-implantation damage in these materials, scanned CW Argon ion laser beams, and incoherent radiation focussed on the sample. Two different but related problems have been addressed. (1) The problem of accurately measuring the equilibrium temperature of the sample in the region that is heated by a focussed CW laser beam has been studied using novel techniques: in-situ high-temperature photoluminescence and Raman-scattering measurements. Accurate temperature measurements for this case have been obtained for the first time; far less spatial dependence of the thermal profiles has been observed than is predicted by existing theories, which neglect important effects such as carrier diffusion. (2) Rapid thermal annealing of ion-implanted InP was studied for a variety of implant and anneal conditions using low-temperature photoluminescence, Raman scattering, and Rutherford backscattering. The results of all three of these characterization techniques were self-consistent, and-

20. DISTRIBUTION / AVAILABILITY OF ABSTRACT ☒ UNCLASSIFIED/UNLIMITED ☐ SAME AS RPT. ☐ DTIC USERS	21. ABSTRACT SECURITY CLASSIFICATION UNCLASSIFIED
22a. NAME OF RESPONSIBLE INDIVIDUAL Thomas G. Ryan	22b. TELEPHONE (Include Area Code) (617) 861-4925 22c. OFFICE SYMBOL RADC (ESO)

DD FORM 1473, 84 MAR 83 APR edition may be used until exhausted
All other editions are obsolete

showed that, in order to obtain single-crystal material with high electrical activation, it is necessary to perform the implants at an elevated temperature (≈200°C) and to anneal at as high a temperature as possible without causing significant dissociation.

TABLE OF CONTENTS

ABSTRACT

The effect of beam-processing on III-V compound semiconductors, particularly indium phosphide (InP), has been investigated in detail. Two types of "beams" have been used to anneal ion-implantation damage in these materials, scanned CW Argon ion laser beams, and incoherent radiation focussed on the sample. Two different but related problems have been addressed. (1) The problem of accurately measuring the equilibrium temperature of the sample in the region that is heated by a focussed CW laser beam has been studied using novel techniques: in-situ high-temperature photoluminescence and Raman-scattering measurements. Accurate temperature measurements for this case have been obtained for the first time; far less spatial dependence of the thermal profiles has been observed than is predicted by existing theories, which neglect important effects such as carrier diffusion. (2) Rapid thermal annealing of ion-implanted InP was studied for a variety of implant and anneal conditions using low-temperature photoluminescence, Raman scattering, and Rutherford backscattering. The results of all three of these characterization techniques were self-consistent, and showed that, in order to obtain single-crystal material with high electrical activation, it is necessary to perform the implants at an elevated temperature (≈200°C) and to anneal at as high a temperature as possible witout causing significant dissociation.

I. INTRODUCTION

This report summarizes the results obtained from an investigation entitled "Minority-Carrier Investigations of Beam-Annealed and Thermally-Annealed Semiconductors" carried out for the Rome Air Development Center during the period October 15, 1981, to October 14, 1984. The material emphasis in this study is on indium phosphide (InP), although some of the investigations have been carried over to other III-V compounds such as gallium arsenide (GaAs), aluminum gallium arsenide (AlGaAs), which has nearly the same lattice constant as GaAs, and superlattice structures formed by growing alternate epitaxial layers of GaAs and AlGaAs. The lattice-matched GaAs/AlGaAs system is currently the best developed material for both optoelectronic devices and high-speed, high-frequency electronic devices (both analog and digital). InP has certain optical and electrical properties that are superior to GaAs, making it (at least in principle) a better candidate for these same device applications. However, far less is known about the fundamental materials properties of InP compared with GaAs and the difficulties involved in processing and device fabrication. The research reported here addresses that problem. In particular, the interaction of InP and other III-V compounds with various forms of energy "beams" (such as laser beams, ion beams, and incoherent radiation focussed onto the sample) is the detailed subject of this work. Much of the research reported here deals with the implantation of electrically-active ion species into these compounds, and the effect of laser or rapid lamp annealing on implant-induced damage and the resulting physical properties of the material after this treatment.

The report is divided into three major sections. First, a brief report is given in Section II of the effect of the heating that takes place when a beam of above-bandgap light is directed onto the surface of a semiconductor.

Due to the strong absorption of this radiation, the heating occurs only in a thin surface layer, causing the activation of the ion implanted impurity; recrystallization of the lattice structure takes place without significant impurity diffusion into the sample volume. It is this heating that is the basis of so-called "laser annealing" or "rapid lamp annealing", considered to be an important processing step after implantation. However, it has proved to be very difficult to measure the temperature produced by lasers or other beams which are used for such annealing. The knowledge of the temperature in the heated surface layer during optical annealing is very important for understanding and controlling the recrystallization process. Due to the small volume of the heated region, especially when focussed laser beams are used, conventional methods of measurement of the temperature cannot be used.

Thus, Section II summarizes a series of experiments dealing with temperature measurements and spectral transformation in these materials. Two spectroscopic methods of temperature measurement have been employed: luminescence and Raman scattering. We have obtained the first reliable temperature measurements during laser beam heating in III-V semiconductors (InP, GaAs, GaAlAs alloy, GaAs-AlAs superlattice). High temperature photoluminescence of III-V semiconductors and the high temperature behavior of the bandgaps were also studied for the first time. A laser-induced transformation of the optical properties of a GaAs-AlAs superlattice was found, and the temperature at which this transformation occurs was determined using a new luminescence technique. This work will be summarized very briefly in Section II, since the results have already been presented in detail in an Interim Report on this project[1] covering the period October 15, 1981, to October 14, 1982.

The process of rapid annealing of the implant damage with an incoherent optical source such as a tungsten/halogen lamp (usually referred to as rapid thermal annealing, or RTA) is the detailed subject of Section III of this report. RTA is emphasized here because of the difficulties encountered during earlier research in producing defect-free InP layers after implantation and laser annealing. We will report a detailed study of the effect of RTA after implantation of donors into InP which is still in progress. Both high and low doses have been studied which, for room-temperature implants, are above and below that required to produce an amorphous layer, respectively. The temperature dependence of the implant conditions has also been studied by carrying out implants at liquid nitrogen temperature, room temperature, and elevated temperatures. Finally, the effect of varying the anneal conditions (i.e., temperature and time of anneal, capping technique, etc.), has been investigated in detail. A significant conclusion of this work is that InP (as well as GaAs and most likely many other III-V compounds) anneals quite differently than silicon (Si) after ion implantation. Our results suggest that single crystal material can be obtained in these compounds only when the amorphous damaged layer is thinner than a certain threshold thickness; above this thickness, polycrystalline material usually results. Three different characterization techniques have been used to investigate the quality of InP after RTA, and each will be discussed in Section III: low temperature photoluminescence, Raman scattering, and Rutherford backscattering. The results described here have been reported in a series of publications.[2-5]

Section IV of this report summarizes the work described in Sections II and III. Sections V and VI list personnel involved in this program, and literature references, respectively.

Finally, Section VII is an important appendix which documents the statement made above that the results obtainable by scanned laser annealing of InP are less than satisfactory. This work was performed on an earlier Air Force RADC contract,* but two papers were written and published[6,7] on this work during the current reporting period. Since the results obtained in these papers are extremely relevant to the RTA studies of InP which are the main theme of the present report, reprints of the papers are attached as an appendix. In the first of these[6] ellipsometry is used to monitor the removal of damage of Se^+-implanted InP after CW scanned laser annealing. The optical extinction coefficient, k, was measured as a function of annealing; a gradual decrease in k as a function of laser power was observed, compared to a very sharp decrease in k for ion-implanted Si, indicating that the ion-implantation damage removal process for InP is more complex than for Si. The second paper[7] investigates the problem of defect formation and electrical activation after Se^+ implantation and scanned laser annealing. Although no impurity redistribution was observed as a result of laser annealing, it was found that the production of arrays of slip dislocations usually accompanied this annealing process, degrading the electrical properties of the implanted and annealed layers. It is believed that slip accompanies the steep thermal gradients which are inherent in the annealing process when using a focussed laser beam; it is for this reason that we have pursued incoherent lamp annealing (i.e., RTA) on the current contract reported here. The results have been extremely encouraging: we have been able to eliminate slip, and preliminary experiments suggest that we can produce good quality layers with high electrical activation.

---

*Air Force Contract F19628-79-C-0128, ROME/RADC, Hanscom AFB.

II. LASER BEAM HEATING AND HIGH TEMPERATURE PHOTOLUMINESCENCE

A. Temperature Measurements

Knowledge of the temperature of the surface of a semiconductor when a laser beam is focused onto that surface is important for laser processing and annealing of semiconductors. Due to the small volume of interaction (resulting from the small size of the laser spot and strong absorption of the radiation within the layer, which is less than 1μm), it is impossible to measure temperature by conventional methods. We have used band-to-band luminescence of several III-V semiconductors excited by the same laser beam which causes heating of a crystal, as a probe of the lattice temperature. Energy position and bandwidth of the luminescence maxima are directly related to the lattice temperature. The temperature dependence of the band-to-band luminescence can be measured with external heating at low-power laser excitation, and can be used as a standard for the determination of the temperature during laser heating. These are the first published results on the photoluminescence of III-V semiconductors for temperatures above room temperature. Therefore, we also studied temperature dependences of the luminescence and the bandgap energy of GaAs and InP, and compared the experimental results with existing predictions and evaluations. There are many theoretical calculations of CW laser beam heating of semiconductors,[8-10] but no reliable experimental measurements. The purpose of this work was to obtain experimental values of the lattice temperature during laser heating. We studied samples of GaAs, InP, $Ga_{0.75}Al_{0.25}As$, and a GaAs-AlAs multiquantum-well structure.

The results of these experiments show that lattice heating is the most important influence on the luminescence spectra for strong CW laser excitation, and that the temperature of the lattice can be determined with high precision due to the high sensitivity of the luminescence band energy to the lattice temperature. The temperature inside the laser spot was measured

as a function of laser power; results for GaAs are shown in Figure 1. The dependence is approximately linear, although the last experimental point shows the beginning of nonlinear behavior, which we believe corresponds to the onset of laser-induced optical damage of GaAs. Very similar results are obtained for InP, as shown in Figure 2.

The temperature inside the laser spot is rather uniform within the beam diameter (measured at 1/e intensity level). This is caused by the diffusion of optically excited carriers and their contribution to the thermal conductivity within the spot. We were not able to measure any difference in the spectra which indicated a difference in the temperature within the spot, even though a magnified image of the laser spot was scanned across the entrance slit of the spectrometer. Details of these measurements are given below.

In comparing our experimental results with theoretical calculations,[9,10] we find that our experiments give lower maximum temperature in the laser spot (Figure 1), presumably because of the contribution of optically-excited carriers to the thermal conductivity. This effect was not considered in the calculations presently available. However, these deviations are not very large in the temperature range considered, because the contribution of optically-excited carriers to the thermal conductivity does not extend much outside of the laser spot.

The temperature profile of the laser spot was measured in a superlattice of alternating layers of GaAs and AlAs, where the GaAs layers were narrow enough to show quantum size effects. This sample was used because the luminescence spectrum of the quantum-well structure consists of an intense, narrow band, which made measurements more accurate. A magnified image of the laser spot was projected onto the screen with a pinhole. The light passing through the pinhole entered the spectrometer and was analyzed. The results

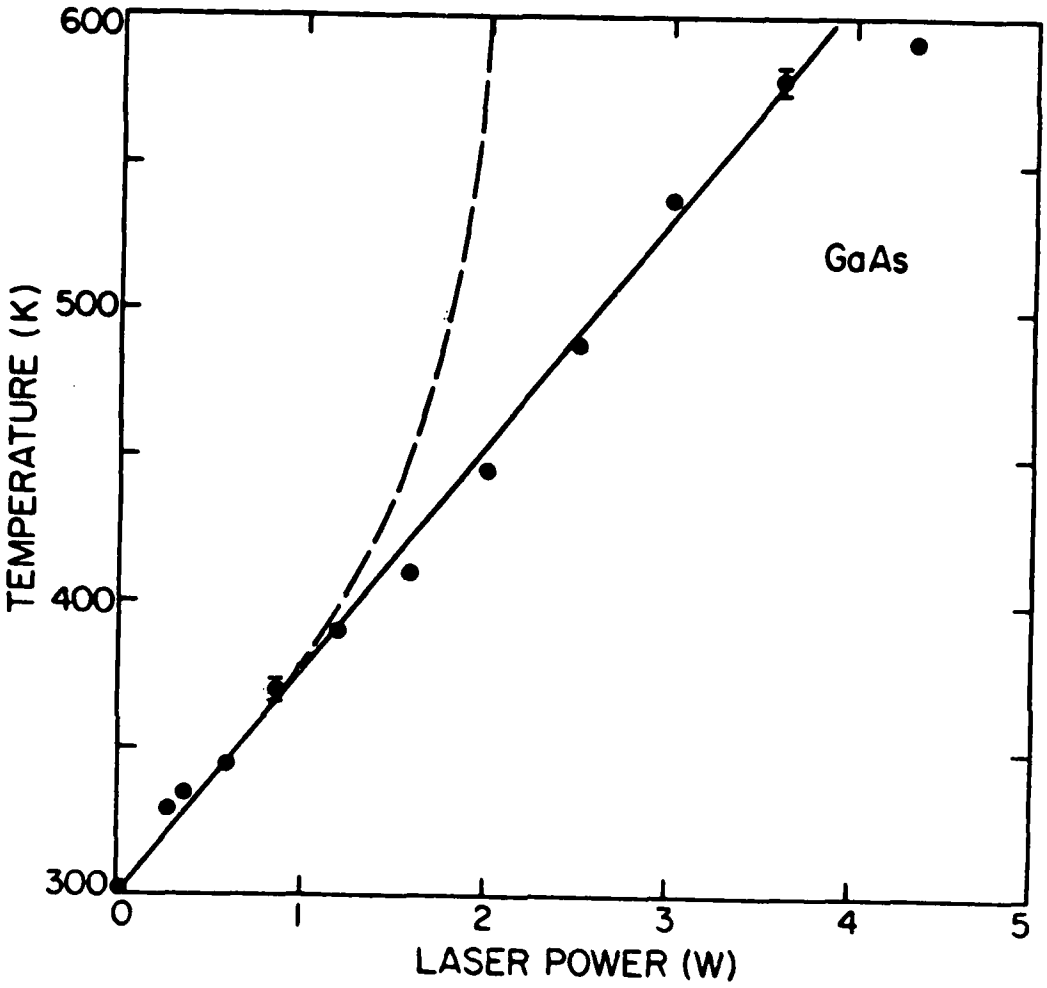

Figure 1. Temperature inside the laser beam spot as a function of the laser power. Laser beam spot diameter ~100μm, GaAs. The dashed line corresponds to calculations.[10]

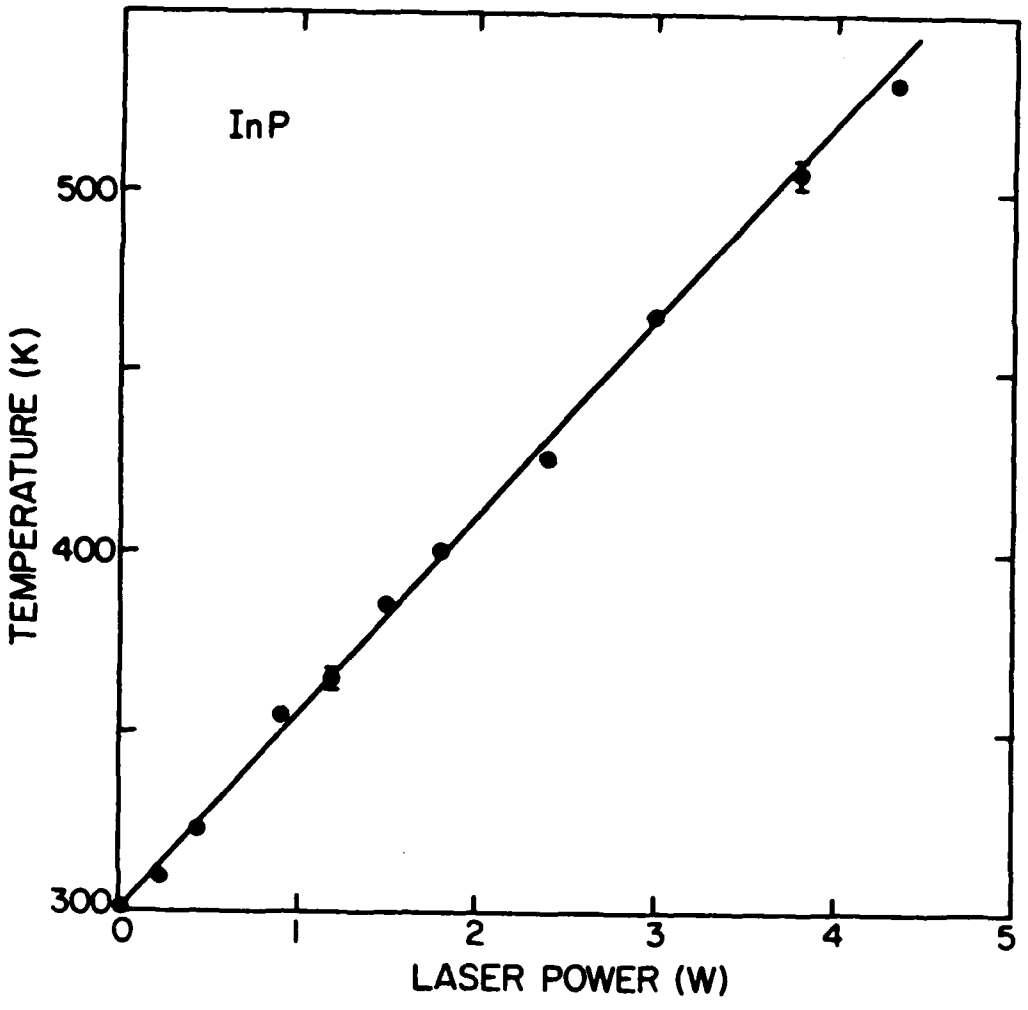

Figure 2. Temperature inside the laser-beam spot in InP, as a function of the laser power. Laser beam spot diameter ~100μm.

obtained are presented in Figure 3. They show that the temperature inside the spot is essentially uniform, in contradiction to most theories. However, available theories do not consider the diffusion of photoexcited carriers and the corresponding increase in thermal conductivity inside the spot caused by this diffusion.

B. Laser-Induced Damage

The temperature inside of the laser spot as a function of laser power was measured for the same GaAs-AlAs quantum-well structure used for the data in Figure 3; the results are presented in Figure 4. Note that the slope of the linear temperature vs. laser power relation sharply decreases in the range of laser power between 1.5 and 2.0 watts. Apparently some sort of structural transformation occurs in this region which requires energy (as is the case for melting), and this reduces the temperature increase.

We found that in this same region the optical properties of the superlattice change in several other significant ways. First, the room-temperature luminescence is nearly quenched. Secondly, the low-temperature luminescence spectrum changes as is shown in Figure 5 by the difference between the solid line (before high-power laser treatment) and the broken line (after). The transition between the n = 1 electron state and the heavy hole state is shifted in energy and slightly broadened by the high-power laser treatment, and the energies of excitonic transitions of the host GaAs material are also shifted. However, the observation of these narrow, shifted quantum well transitions, along with the narrow excitonic transitions of GaAs, suggests that the transformation of the GaAs-AlAs superlattice is not a simple disordering of the layers induced by the laser processing, but instead must be some type of ordered transformation (for example, an ordered array of dislocations, or periodic strain fields which reduce the transition energy

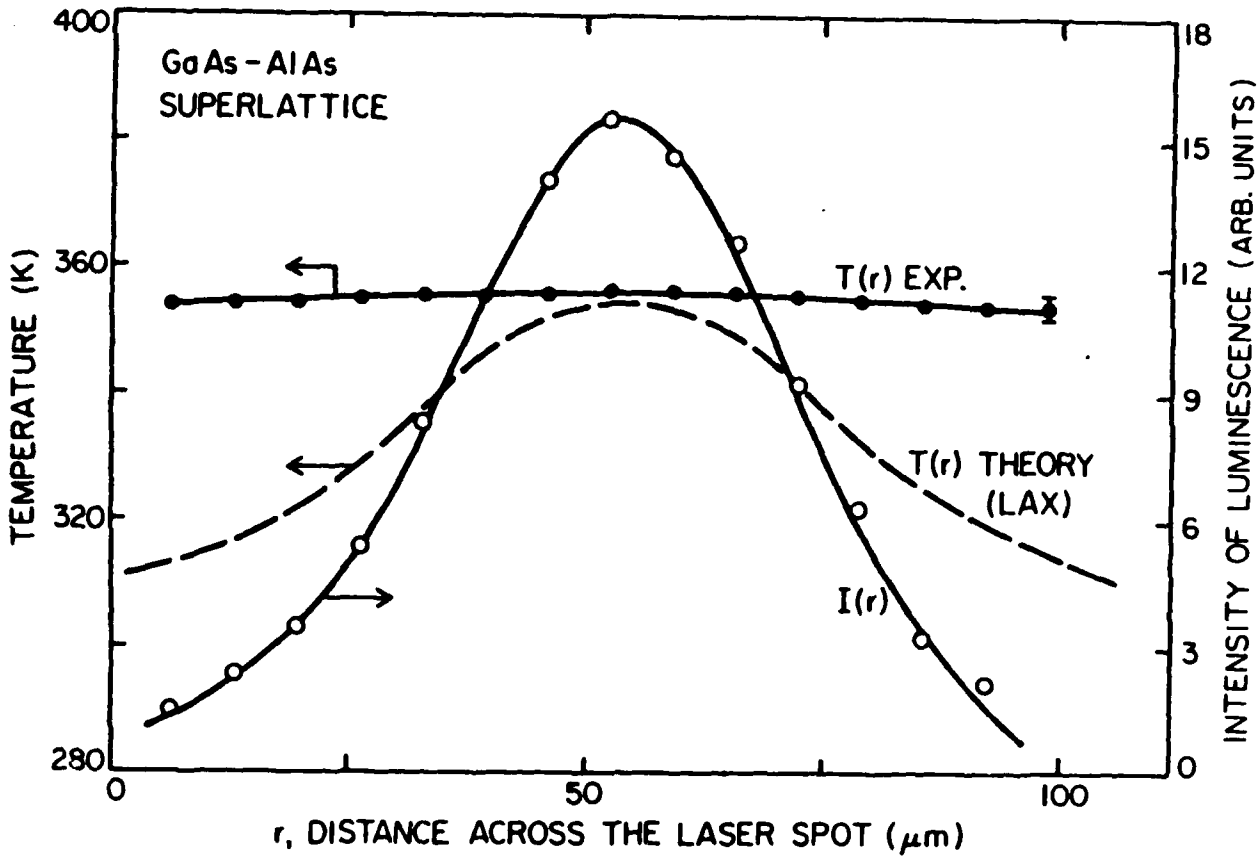

Figure 3. Temperature distribution T(r) in GaAs-AlAs superlattice across the laser spot. Points are experimental data, dashed line corresponds to the theory.[8] Distribution of the luminescence intensity I(r) across the spot (circles are experimental data) is also shown.

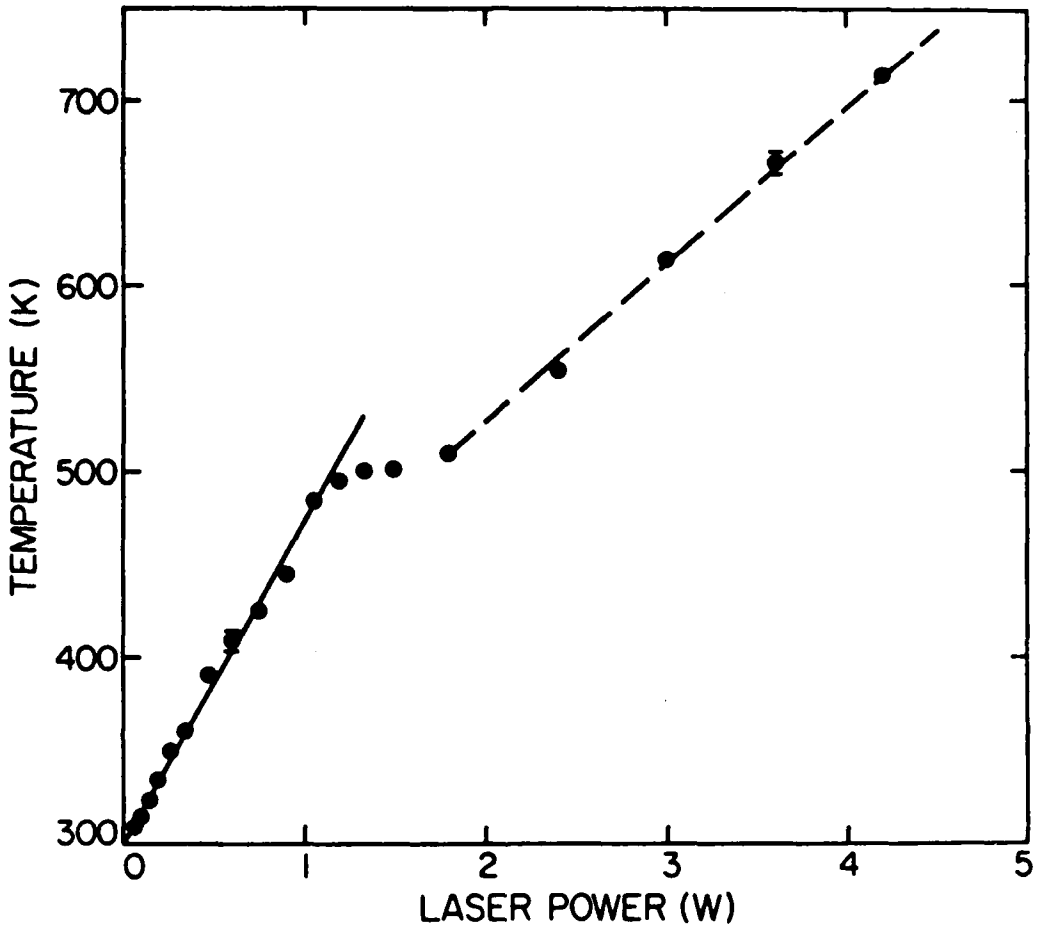

Figure 4. Temperature inside the laser-beam spot for a GaAs-AlAs superlattice as a function of the laser power. Laser beam spot diameter ~100μm.

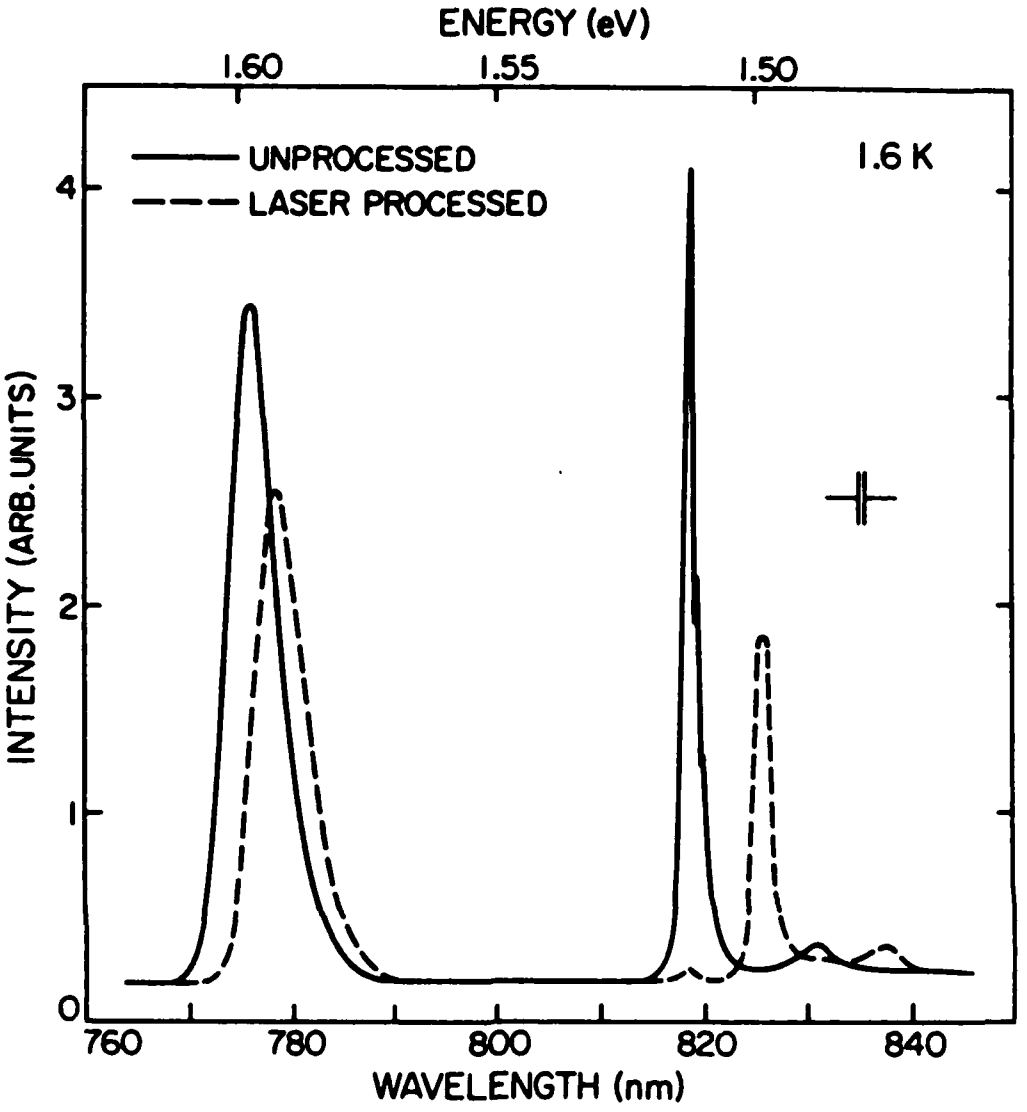

Figure 5. Low temperature (1.6K) luminescence spectrum of the GaAs-AlAs superlattice. The continuous line corresponds to the original superlattice, the broken line to the laser-processed superlattice.

only slightly). Structural studies, such as transmission electron microscopy, are needed before the actual mechanism for these changes can be identified.

Further study of this phenomenon could be very important, since GaAs-AlAs quantum-well superlattices have unusual optical and electrical properties which make them of great interest for new classes of semiconductor devices. Laser processing of these superlattices may prove to be an important technique for device fabrication. However, little work has been done to date to explore the effect of beam processing on these unique materials. We have found that the superlattice cannot be melted or inter-diffused by the laser beam to form a GaAlAs ternary alloy without first producing substantial mechanical damage. At a certain threshold before destruction of the sample a new "phase" of the superlattice is formed, as is clear in Figure 4, with quite different luminescent properties. The threshold for this transformation is ~240 W/cm^2, corresponding to a sample temperature of ~500 K, measured using techniques described above. The details of both the temperature determination and the laser-induced damage experiments have been published.[11,12]

III. RAPID THERMAL ANNEALING OF ION-IMPLANTED InP

As described in the Introduction, considerable attention was devoted during this research program to the rapid thermal annealing of implant damage. Three powerful and complementary characterization techniques were utilized to understand the nature of the recrystallization process: low temperature photoluminescence (PL), Raman scattering (RS), and Rutherford backscattering (RBS). Additional measurement techniques, such as electrical data and capacitance or carrier profiling, are currently underway under a new Air Force ROME/RADC research grant and will be reported elsewhere.

A. Experimental

The undoped samples of InP used for the present studies were highly polished [100] wafers ~300μm thick, and were n-type with a free carrier concentration at room temperature of $1.22\times10^{16}cm^{-3}$. The samples were implanted with Si^{+} ions at a dose of $3.3\times10^{14}cm^{-2}$ and energy of 180 keV. In order to avoid channeling, the samples were oriented with the [100] axis at an angle 7° to the ion beam direction. The samples were held at either liquid nitrogen temperature, room temperature or 175°C during implantation. The purity of the ^{28}Si beam was monitored before and after implantation by checking the ratio of the mass 28 to mass 29 beam intensities; however a small contribution of N_2 (<5%) to the total implantation cannot be excluded. After implantation the samples were capped at room temperature with a cathode-sputtered film of SiO_2 ~100nm thick and were annealed using the Heatpulse system of A.G. Associates.[13] The samples were placed face down on a Si wafer and both sides of the sample were heated by lamps in an inert Ar atmosphere. The annealing temperature and time profiles were measured using a thermocouple cemented onto the Si wafer. Different annealing cycles could be chosen using the computer

control of the Heatpulse system. Maximum annealing temperatures and times were limited by melting of the sample.

The luminescence spectra were recorded using a 1m spectrometer, cooled Ge detector and lock-in amplifier. Low power (~20mW) weakly focussed argon laser radiation with a wavelength 514.5 or 488μm was used for the excitation of the luminescence. The exciting radiation was absorbed in a surface layer less than 200nm thick; the luminescence therefore probed only the implanted part of the sample, since the projected range of Si^+ ions in InP at 180 keV is ~200nm. Low temperature measurements were done at 1.8K with samples immersed in superfluid He pumped below the lambda point, or with samples suspended in the He gas for variable temperature measurements. We found very little difference in the optical spectra before and after cap removal. Most of our results were obtained on samples with caps.

Raman spectra were recorded using the same single-pass spectrometer as was used for luminescence, equipped with an I_2 cell 21 cm long, heated to 100°C, which strongly absorbed the elastically scattered incident light. An intracavity etalon was inserted into the laser cavity for single mode operation, and the laser frequency was tuned precisely to the overlapping P(13) and R(15) lines in V'' = 0 to V' = 43 $^1\Sigma^+_{og} \rightarrow {}^3\Pi^+_{ou}$ transition in I_2 vapor in the region of 514.5nm.[20] Raman spectra were measured also with a triple Cary 82 spectrometer. Raman spectra could be recorded on samples only after cap removal, because the caps emitted a stronger luminescence background than the Raman signal.

B. Photoluminescence

Important information on the rapid lamp annealing of ion-implanted semiconductors may be obtained by means of optical spectroscopic diagnostics. The attractive features of this diagnostic technique are its nondestructive

character and the possibility of obtaining specific detailed information about some or all of the following phenomena: the reconstruction of the crystalline structure, the elimination of defects, the activation of electrically-active impurities introduced by ion implantation, and the optimum annealing temperature. Since photoluminescence (PL) is a minority-carrier effect, the observation of efficient radiative recombination associated with substitutional impurities is usually a much more sensitive measure of the electrical activation of donors and/or acceptors than the more standard majority-carrier measurements such as sheet resistivity. In amorphous or strongly disordered material, many defect states are present in the forbidden gap; these deep defect levels are effective steps in one-phonon nonradiative recombination of photoexcited carriers, so that radiative recombination is quenched. The same defects limit the lifetime and mobility of free carriers, adversely affecting the properties of devices made from this material, particularly minority-carrier devices. Only in sufficiently high quality samples with a low concentration of deep levels can room temperature band-to-band luminescence be expected to appear. In this case, nonradiative relaxation processes require the simultaneous participation of many phonons, and therefore have low probability. In addition to the intensity, the lineshape of band-to-band luminescence may characterize the free carrier concentration and shallow defect states in the annealed sample. We have studied in detail the band-to-band PL of ion-implanted InP after rapid lamp annealing, including the influence of different implant and lamp annealing conditions.[3,4]

1. Low Temperature Luminescence

The low temperature PL spectrum of virgin InP is shown in Figure 6(b). The maxima in the spectrum may be interpreted as follows.[14] The line A at ~1.417eV corresponds to transitions involving excitons bound to donors. The

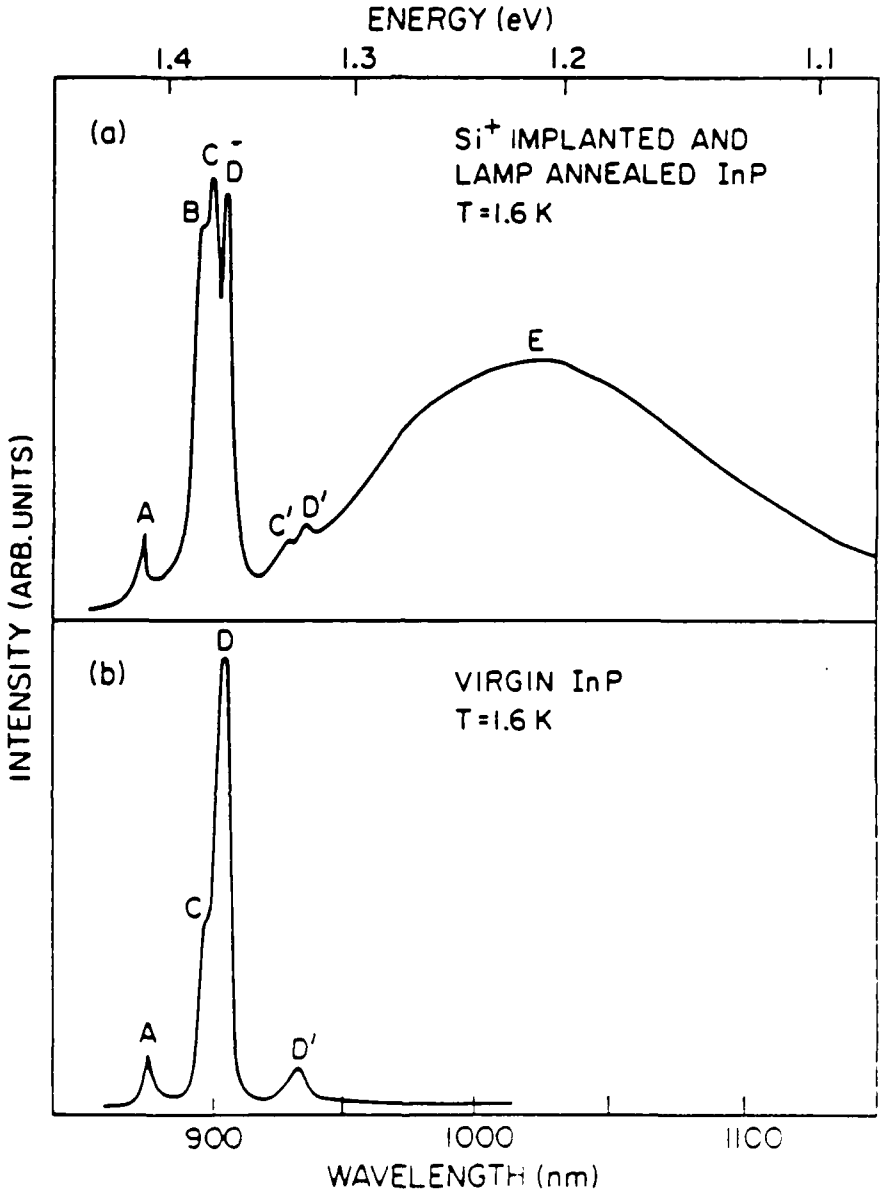

Figure 6. (a) Low temperature (T = 1.8K) PL spectrum of InP hot implanted and lamp annealed at 900°C, 5 seconds.

(b) The spectrum of virgin InP. The assignment of maxima is given in Table I.

shoulder C at 1.377eV and the maximum D at 1.369eV correspond to donor-acceptor pair recombination, and D´ (1.327eV) is the first LO-phonon replica of D. All these peaks are usually seen in undoped InP, and are associated with commonly present unidentified defects.

Ion implantation at low or elevated temperatures produced a large number of defects which were effective centers for nonradiative recombination of photo-excited carriers; neither low temperature nor room temperature PL could be detected after implantation. The same effect was observed after Rutherford backscattering (RBS) analysis of the samples, presumably because of the 2 MeV beam of H^{++} ions. Only after thorough annealing could the band edge or impurity luminescence be detected. The PL spectrum of an InP sample implanted with Si^{+} ions at 175°C (i.e., hot implant) and lamp annealed under optimal conditions[15,16] for 5 seconds at 900°C is shown in Fig. 6a. New features appear in the spectrum of Figure 6(a) in comparison with Figure 6(b). A broad maximum E at ~1.22 eV appears which was observed earlier in Si doped InP.[17] This band may correspond to transitions between free or weakly bound electrons and deep Si acceptors formed from substitutional Si at P sites. The maximum C and its LO phonon replica, C´, are stronger in intensity than in a virgin sample, and a new maximum B at 1.381eV, which has not been observed earlier, appears in the spectrum 6(a). Because the B maximum appears only in well-annealed Si-doped material, it may be associated with a Si impurity; a possible mechanism would involve the transitions between the Si-donor and unidentified acceptor states. The peak C, coincident in energy with the shoulder C in the virgin sample, increases dramatically after Si implantation and annealing; it is conceivable that this results from another Si donor-acceptor pair recombination. The energies of these luminescence transitions and the interpretations suggested above are summarized in Table 1.

TABLE I

Low temperature luminescence bands, their energies and assignment

Band	Energy (eV)	Assignment
A	1.417	Excitons bound to donors
B	1.381	Si donor-acceptor pair transitions
C	1.377	Si donor-acceptor pair transitions
D	1.369	Donor-acceptor pair transitions
C´	1.335	LO replica of C
D´	1.327	LO replica of D
E	1.215	Free or weakly bound electrons to deep Si acceptors

The transformation of the low temperature spectrum of hot-implanted InP (implantation temperature 175°C) with increasing time of lamp annealing at 850°C is illustrated in Figure 7. As the annealing time (and hence quality of the annealing) increases, the intensity of lines A, C, and D increases, showing significant improvement of the sample quality and the elimination of defects. The new features B and E, characteristic of Si doping, appear only in better-annealed samples.

The low temperature spectra of lamp-annealed samples that have been implanted at room temperature are shown in Figure 8. In this case, as Raman data show,[5] the surface layer is made amorphous by implantation, unlike the hot-implant case, for which it remains single-crystalline with a high density of defects. The spectrum in Figure 8(a) corresponds to the optimum annealing case. Annealing for 20 seconds at 850°C gave a similar spectrum. It is important to note that the line B and the broad band E, which are present in the hot-implanted sample, are absent in this case, suggesting that the majority of Si atoms are non-substitutional due to incomplete reordering of the amorphous layer. Let us note also that the bound exciton maximum A is a sensitive probe of the crystalline quality. It is absent in the partially annealed sample, Figure 8(b), and grows in intensity with improved annealing.

The low temperature spectra of implanted samples annealed in the conventional manner (i.e., oven annealing) at 775°C for 15 minutes are given in Figure 9. These conditions are close to optimal for oven annealing.[15] Band E, corresponding to deep Si acceptor levels, is absent in the spectrum of the room temperature implanted sample, Figure 9(b), showing that the activation of Si impurities is far from complete. However, band E has strong intensity in the spectrum of the hot-implanted, oven-annealed sample Figure 9(a); nevertheless this spectrum differs from the spectrum of the lamp annealed sample,

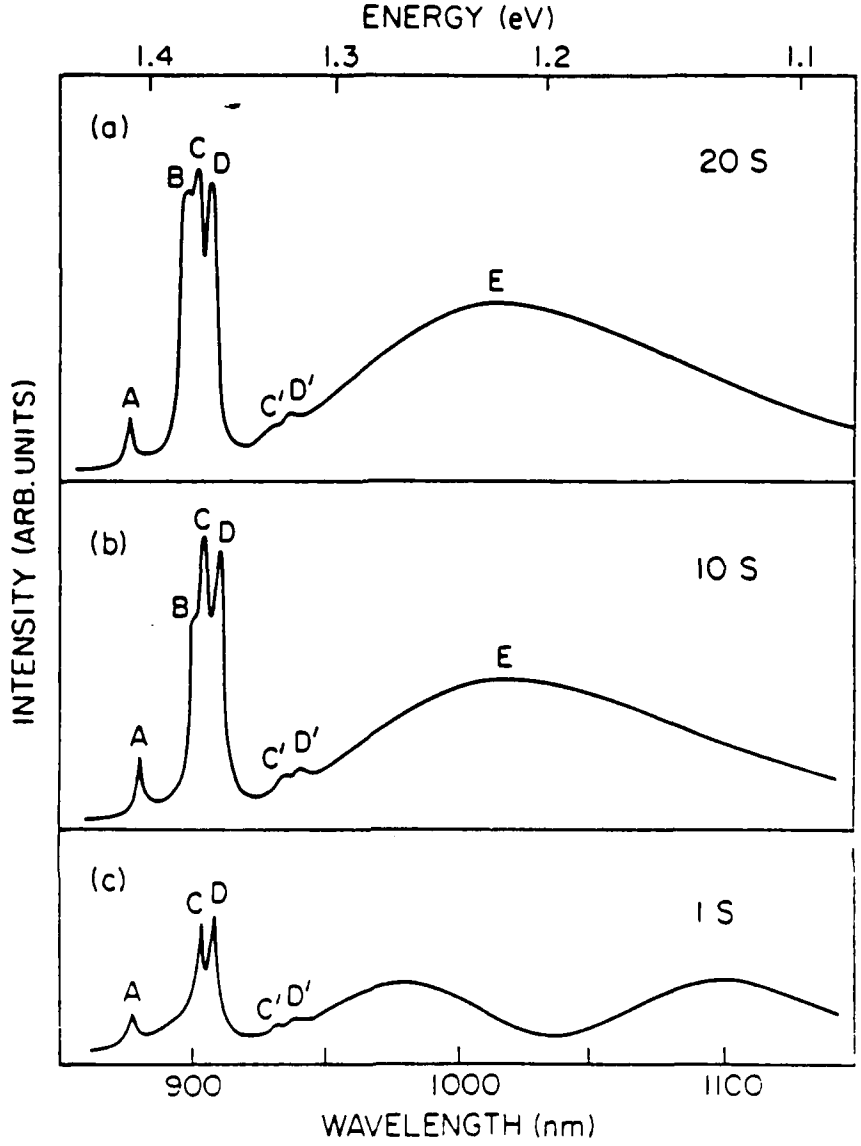

Figure 7. Low temperature spectra of hot implanted InP annealed by lamp at T = 850°C during (a) 20 seconds, (b) 10 seconds, (c) 1 second.

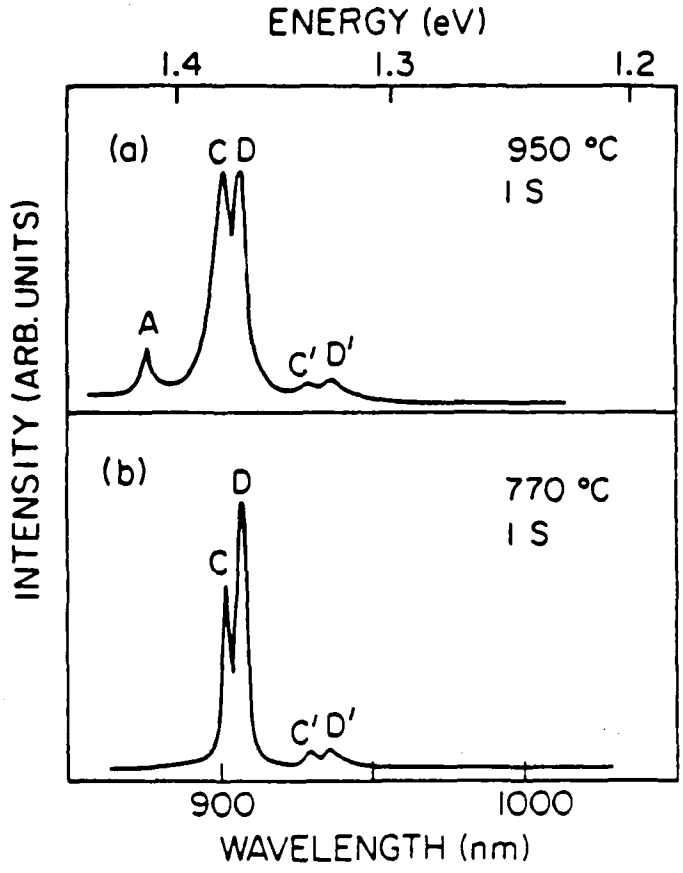

Figure 8. Low temperature spectra of room temperature implanted InP lamp annealed during 1 second at (a) T = 950°C and (b) T = 770°C.

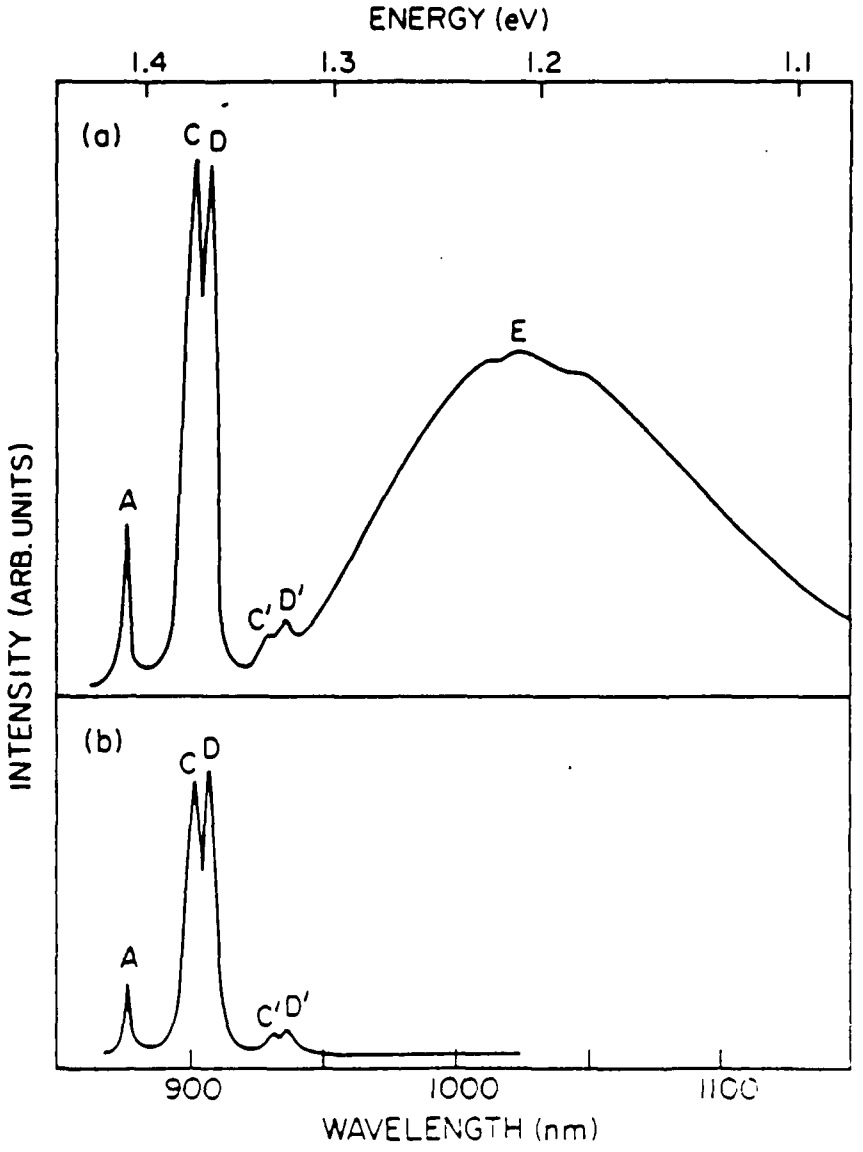

Figure 9. Low temperature spectra of (a) hot implanted and (b) room temperature implanted InP after annealing in an oven.

Figure 6(a), in one important respect: line B, which we attribute to transitions between Si donors and shallow acceptors, is absent in the oven-annealed sample. This suggests that the activation of Si impurities is worse in the case of oven annealing.

The spectra of lamp and oven annealed samples implanted at liquid nitrogen temperature were similar in structure to the spectra of room temperature implanted samples but the quality of those samples after annealing was even worse.

2. Room Temperature Luminescence

As is evident from the low temperature spectra, the shallow Si donors were not ionized at 1.6K in implanted and annealed samples at our doping level. The bound exciton transitions had the same energy as in a virgin sample and there were no signs of influence of free carriers on the spectra. This is consistent with known values of the ionization energies of shallow donors in InP, approximately 5-6 meV.[14] In the case of room temperature spectra all shallow donors are ionized and the annealed material may become degenerate. This could lead to an increase of the effective bandgap due to the Burstein-Moss effect. Room temperature PL spectra of the hot implanted samples lamp annealed at 850°C for different time intervals are shown in Figure 10. The room temperature spectrum of a virgin sample is also shown for comparison. Two maxima are present in the spectra of annealed samples. The maximum at ~1.15eV corresponds to band E at ~1.22eV in low temperature spectra and is believed due to transitions between free electrons and deep Si acceptors produced by Si atoms at P sites.[17] The peak at ~1.35eV corresponds to band-to-band transitions. It broadens and shifts towards higher energy with increasing anneal time; this is particularly evident when implanted and annealed samples are compared with virgin material. These changes are caused mainly by activated free carriers in the conduction band.

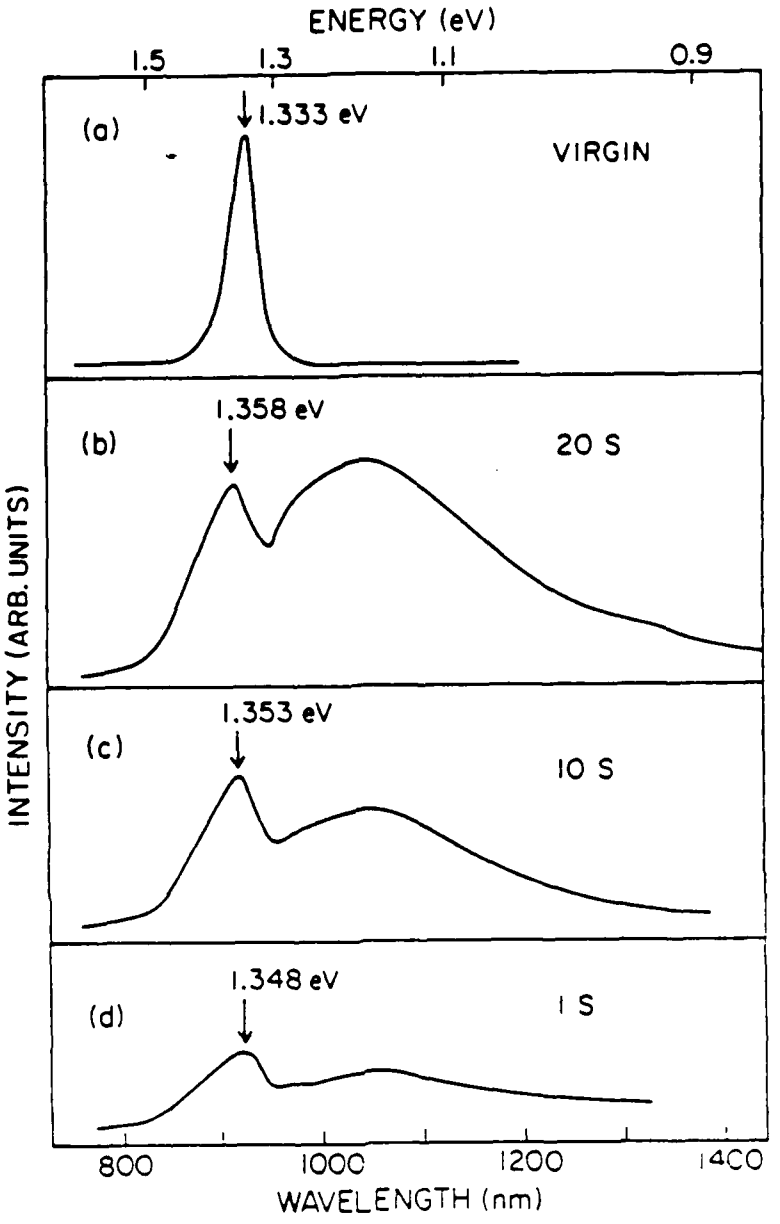

Figure 10. Room temperature spectra of (a) virgin and (b)-(d) hot implanted and lamp annealed at 850°C InP with anneal time of (b) 20 seconds, (c) 10 seconds, and (d) 1 second. Note the increase of the energy of the band-to-band PL maximum due to increase of free electron concentration in a conduction band.

The shift of the luminescence maximum to higher energies is a manifestation of the Burstein-Moss effect, which takes into account the filling of band states under conditions of high carrier density. This effect is much stronger in InP for n-type doping because of the low density of states in the conduction band. The dominating transitions in this case of heavy doping occur between the electrons near the Fermi level in the conduction band and holes in the impurity tail of the valence band. This increased concentration of electrons in the conduction band contributes to the Fermi level shift to higher energy and the corresponding increase of the effective bandgap. At the same time, bandgap shrinkage occurs due to the growth of the impurity induced tail of the valence band. The concentration of free carriers may be evaluated from the experimentally measured luminescence energy shift,[18,19] keeping in mind the two competing effects described above. Thus, for the highest energy shift observed, ~25meV as seen in Figure 10(b), the corresponding concentration of activated carriers is $\sim 3\times10^{18}$ cm^{-3}.[19] Note that the increase of PL intensity and the shift of the bandgap luminescence with increasing anneal time, which is discussed above and which can be seen in the spectra of Figure 10, illustrate the improvement in the quality of the sample after suitable annealing.

The room temperature spectra of hot implanted (a) and room temperature implanted (b) samples oven annealed at 775°C for 15 minutes are compared in Figure 11. As can be seen, the quality of the hot implanted sample is much better than that of the room temperature implanted sample. The latter shows only some unidentified deep-level PL without traces of band-to-band PL. The energy of the band-to-band PL maximum in Figure 11(a), 1.348eV, is shifted towards higher energies in comparison with a virgin sample, 1.333eV, but the shift is smaller than in the case of lamp annealing under optimal conditions,

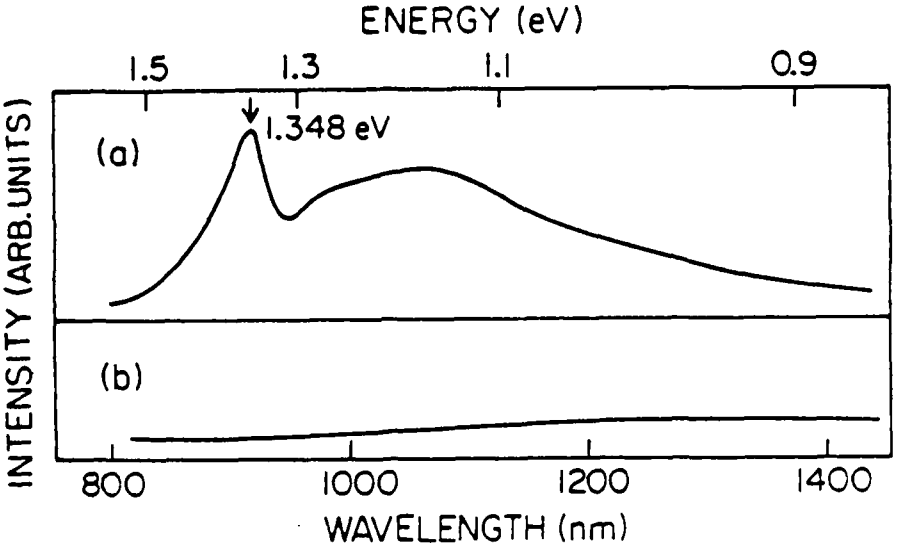

Figure 11. Room temperature spectra of (a) hot implanted and (b) room temperature implanted InP after annealing in an oven.

Figure 10(b). Note that oven annealing results in a spectrum very similar to lamp annealing for 1 second at 850°C only. This shows that lamp annealing of hot implanted samples at optimal conditions produces a larger concentration of free electrons in the conduction band than optimal oven annealing.

PL spectra of room-temperature implanted samples subjected to 1 second lamp annealing at different temperatures are shown in Figure 12. As can be seen, the intensity of band-to-band PL with peak energy in the range of 1.35 eV rapidly increases with increasing annealing temperature (and increasing sample quality). The large width of this band-to-band PL band, and the detectable energy shift, both show that free carriers are introduced into the conduction band by implantation and annealing. The lower energy position of the band-edge PL (E = 1.348eV) and absence of the Si deep acceptor band in comparison with the hot-implanted sample annealed using similar "optimal" conditions (E = 1.358 eV) show that it was impossible to anneal the room temperature implanted InP to the same degree of perfection as hot implanted InP. This agrees with the low temperature PL results.

C. Raman Scattering

The room temperature Raman scattering (RS) spectra of samples implanted at different fluences of Se^+ ions at 390keV and 200°C are shown in Figure 13. Note the increase of disorder which is manifested in the breakdown of normal selection rules (the intensity of the TO-mode is prohibited in the back scattering configuration along the [100] crystal direction and is seen in Figure 13(a) only because of the non-zero solid angle used to collect the scattered light), broadening and shifting of the peaks, and the appearance of disorder-induced broad band scattering. The crystalline phase is conserved even for the highest implantation doses for hot implantation which can be deduced from the presence in the spectra of well resolved LO and TO zone-center phonons.

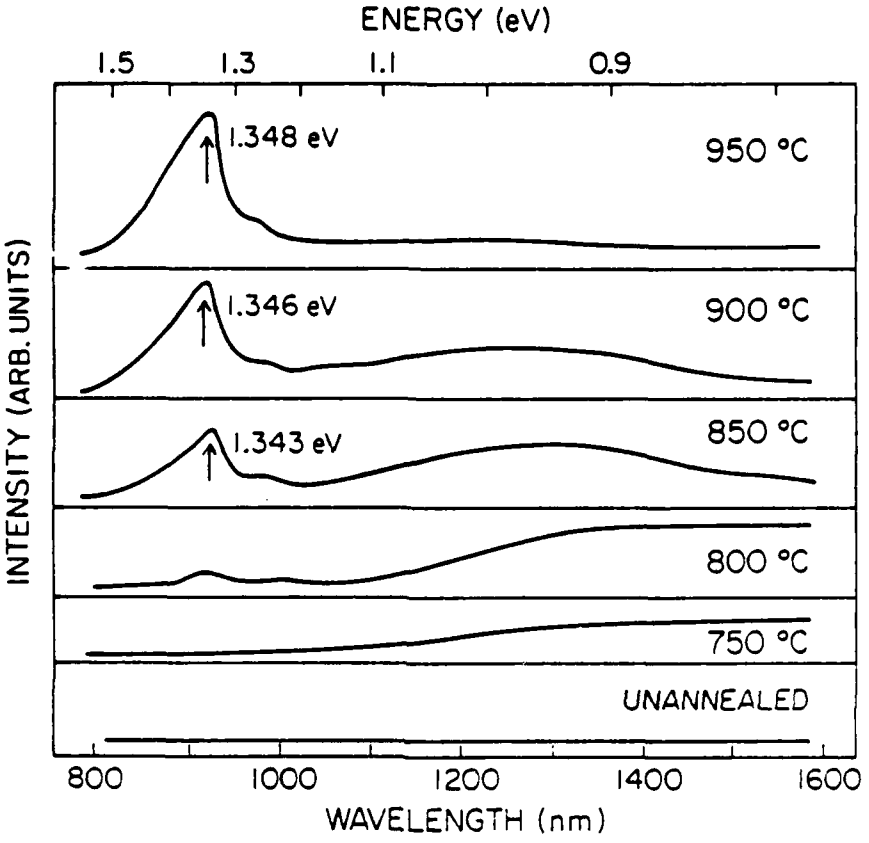

Figure 12. Room temperature PL spectra of room temperature implanted and lamp annealed samples. Annealing temperature is shown. Annealing time was 1 second for all cases. Note the increase of the energy of the band-to-band PL maximum due to increase of free electron concentration in a conduction band.

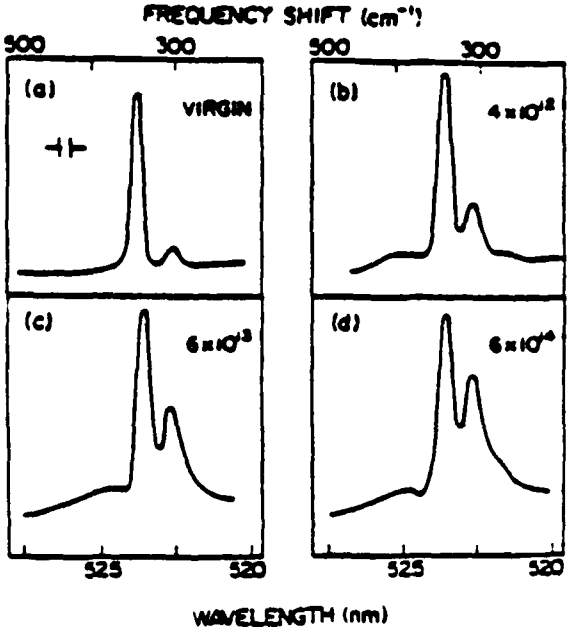

Figure 13. Room temperature Raman spectra of InP implanted to different doses.

The transformation of the spectrum of ion implanted InP (dose $6\times10^{14}cm^{-2}$ Se^{+} at 390keV, hot implantation) during heating in the oven is shown in Figure 14. Note that disorder starts to decrease at 200°C and the crystalline order is much improved at 430°C. The implanted layer is very close to single crystal at this temperature. Shift and line broadening due to heating are also present in the spectra.

RS of InP implanted at room temperature by Si^{+} ions at a dose $3.3\times10^{14}cm^{-2}$ at 180keV are shown in Figure 15. The spectra obtained after 1 second lamp annealing at different temperatures are also shown. Note that ion implantation at room temperature produces amorphous InP. The spectrum of the unannealed sample corresponds to the one-phonon density of states of InP[21,22] and does not show LO and TO zone-center phonons. This is a characteristic feature of the amorphous state. The lowest annealing temperature, 750°C, restores crystalline order, as evidenced by the appearance of both LO and TO phonons. However, the strong TO phonon intensity in this configuration (for which TO is prohibited) suggests that the annealed layer remains polycrystalline even after the highest temperature annealing (950°C). Lamp annealing with times as long as 30 seconds, or traditional oven annealing at 775°C during 15 minutes, did not produce single crystal material, as evidenced by the strength of this forbidden Raman line. From this it is possible to conclude that annealing of ion implanted amorphous InP is not a solid phase epitaxial growth from the substrate, but that the recrystallization is to a large degree independent of substrate orientation. Hot implantation of InP, on the other hand, preserves the crystalline structure of the layer (though it is highly defective), so that there is remaining structure for preferential single crystal growth. This result may also be valid for other semiconductors, and is noted here for the first time. This resulting polycrystalline structure of room temperature implanted and annealed InP layers is probably

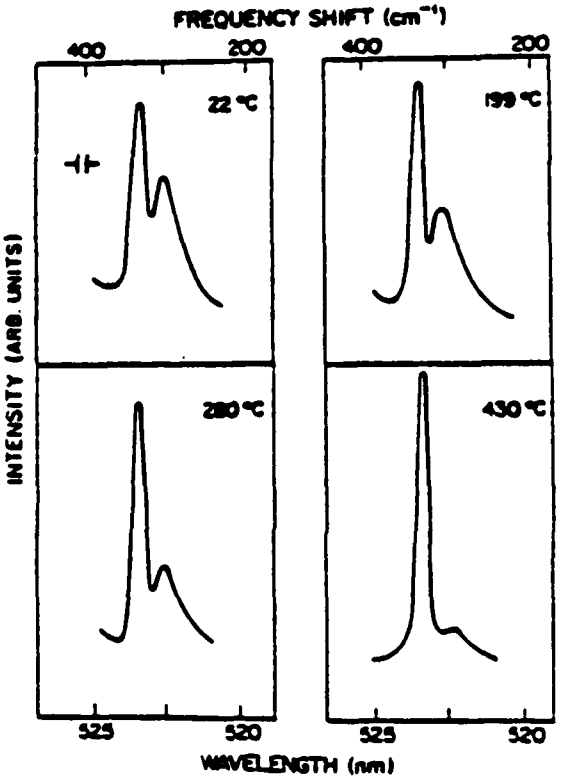

Figure 14. Transformation of Raman spectrum of InP implanted at $6\times10^{14}cm^{-2}$ Se^{+} at 390keV and 200°C during annealing in an oven.

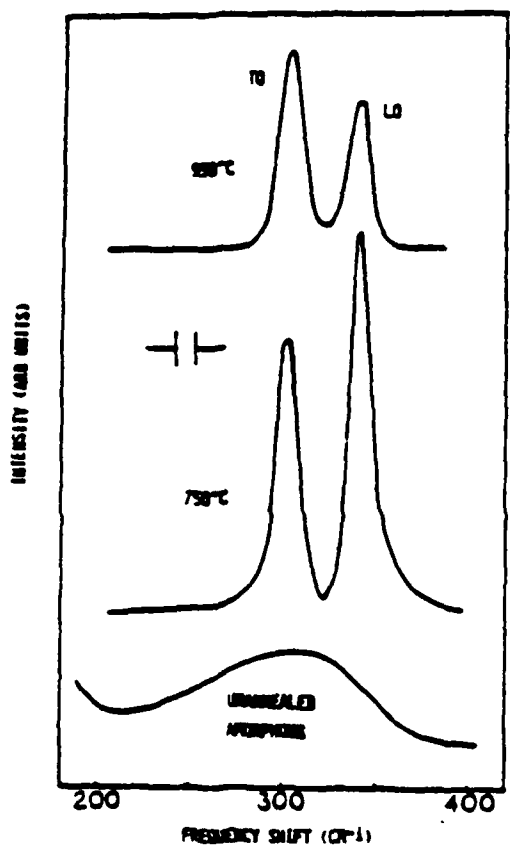

Figure 15. Room temperature Raman spectra of InP implanted at 3.3×10^{14} cm^{-2} at 180 keV and 20°C after 1 second lamp annealing.

the cause of the higher resistivity and lower mobility[8] of these samples in comparison with hot implanted samples.

Additional room temperature RS spectra are shown in Figure 16. Only the LO-phonon line at 347.5 cm^{-1} allowed by selection rules is present in the spectrum of a virgin sample, Figure 16(a). The prohibited TO-line at 308 cm^{-1} is hardly seen. The spectrum in the same scattering configuration of the hot implanted sample ($3.3x10^{14}$ Si^{+} cm^{-2}) after lamp annealing at 850°C for 20 seconds is shown in Figure 16(b). All well annealed (by a lamp or in a furnace) samples implanted at room temperature or at 175-200°C have similar Raman spectra. A new line coincident in energy with TO phonons appears in the spectrum. This line is expected to appear in Raman spectra of highly doped InP, due to formation of phonon-plasmon coupled modes (L^{-} mode).[23] We consider the free carrier contribution to this line to be dominant. As our data have shown, the hot implanted sample remains single crystal after the implantation dose used in the present work, and the intensity of the prohibited TO mode remains small after implantation. Though low temperature annealing produces noticeable improvement of crystalline structure,[2] only high temperature annealing produces activation of carriers and growth of the plasmon-phonon line. We were not able to detect unambiguously plasmon excitations of the higher energy branch, which allows a determination of the carrier concentration and mobility,[23] most probably due to strong damping of plasmons due to defects. The expected position of this plasmon line for the spectrum in Figure 16(b) was in the range of 950 cm^{-1}.

The spectrum of the unimplanted sample capped and annealed at 900°C for 5 seconds is shown in Figure 16(c). As can be seen from the figure, the spectrum is quite similar to that of the virgin sample. Therefore, it may be concluded that annealing at conditions close to melting conserves the single-crystal structure of the sample surface.

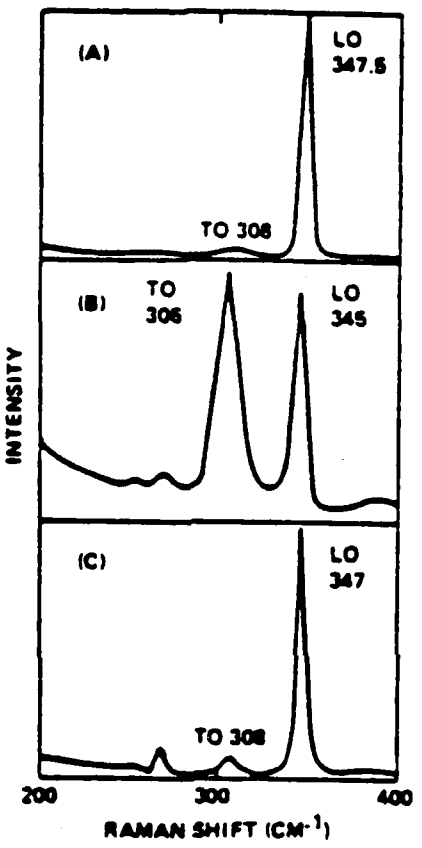

Figure 16. Room temperature Raman spectrum of InP; (A) virgin sample; (B) hot implanted InP after lamp annealing at 850°C during 20 seconds; (C) unimplanted InP after lamp annealing at 900°C during 5 seconds.

In summary Raman data showed that the layers implanted at room temperature were amorphous after implantation and could not be restored to a single crystal state by lamp, oven or CW laser annealing. The only anneal state that could be obtained was apparently polycrystalline. Annealing of hot-implanted samples, on the other hand, which preserved their crystalline nature after implantation, produced single crystal material with good carrier activation.

D. Rutherford Backscattering

The nature of implantation-induced damage in InP as a function of implantation and substrate variables has also been investigated using Rutherford backscattering (RBS), as a complementary method to the PL and RS described in Sections III B and C above. The motivation for these studies is the ability of RBS to directly detect crystalline damage (although its sensitivity to defects is considerably lower than in the case of PL and RS). RBS has shown that the nature of the residual damage after ion implantation is a strong function of implant and substrate variables. The implantation variables of particular interest are the total dose, dose rate, and the mass and energy of the incident ions. The important substrate variable is the temperature during implantation. In particular, we are interested in studying the effects of different annealing conditions on the recrystallization and electrical activation of implanted dopants.

The conventional method of removing ion implantation damage involves isothermal annealing treatments in a furnace in the temperature range of 700-800°C for 15-30 minutes. Recently more advanced RTA methods have developed for removing implantation damage. It appears from all of the data reported here that the nature of the ion-implantation damage before annealing determines the amount of residual damage, electrical activation, and mobility achieved after annealing, for both conventional and advanced annealing methods.

The RBS measurements reported here are preliminary in nature, since they have just been initiated near the end of the contract period covered in this report. For this reason, the actual RBS and channeling data will not be presented in this report, but the results of some of the measurements obtained at Stanford University in collaboration with T. W. Sigmon and J. R. Abelson will be briefly described. These preliminary data appear to be consistent with the annealing results obtained using PL and RS, as described above.

Random and (100) aligned backscattering spectra of InP samples implanted with 180 keV Si ions at room temperature with fluences from 10^{13} to 10^{15} ions/cm^2 have been measured. At a fluence of 10^{14} ions/cm^2 the aligned spectrum coincides with the random spectrum in the near surface region, indicating that the crystal has been disordered to a depth of about 2500Å as measured by this technique. As the implanted dose is further increased the amorphous-crystalline boundary expands. The layer retains some crystallinity for implants of 5×10^{13}ions/cm^2. The limit of sensitivity for damage detection was found at a Si implant level of 10^{13}ions/cm^2. Layers that were disordered from implantation were still disordered after one year.

For 180 keV 3.3×10^{14}ions/cm^2 as implanted and after furnace annealing at 750°C for 15 minutes or rapid thermal annealing at 850°C for 5 seconds, the sample was epitaxially regrown from the interior interface between the damaged layer and the bulk crystal, but a thin highly disordered region was left. Increasing the FA time to 60 minutes or the RTA to 20 seconds did not change these results.

A comparison of the results for "hot" implants (180 keV, 3.3×10^{14} and 10^{15}ions/cm^2 implants at 200°C) indicates that there is a little residual crystalline disorder generated for the "hot" implant for a fluence which would produce an amorphous layer in a sample held at room temperature. After RTA

the disorder lowers to a level similar to that of unimplanted wafer. FA is unable to anneal the small amount of residual damage that is left after "hot" implants. No significant difference was found between capped and capless annealing.

In summary, our results show that the annealing behavior of the amorphous layer created by Si implantation into InP is considerably different from that for Si.[24] In the case of Si, an amorphous layer produced by ion implantation can be recrystallized to form good quality single-crystal material by solid phase epitaxy, with good electrical activation. InP, on the other hand, behaves like GaAs:[24,25] For RT implantation, the damage recovery following FA or RTA depends on the thickness of the amorphous layer. The maximum epitaxial regrowth thickness is about 2000Å. For implantation at 175-200°C self-annealing reduces crystalline disorder to a low level even at high doses. RTA following hot implants further reduces the damage level to that of an unimplanted wafer.

IV. SUMMARY

The following results have been obtained on this research contract:

A. The first reliable measurements have been made of the true temperature of the surface of compound semiconductors during CW scanned laser annealing, using high temperature PL. The temperature as a function of laser power was found to be linear for InP and GaAs. For the case of a GaAs/AlAs superlattice sample, a laser-induced transformation of the superlattice was observed, and the temperature at which this transformation occurs was accurately measured.

B. Rapid thermal annealing (RTA) of ion-implanted InP was studied for a variety of implant and anneal conditions using photoluminescence, Raman scattering, and Rutherford backscattering. The results of all three of these techniques were consistent, and present a picture that good recrystallization and the elimination of damage occur only for optimal conditions: high temperature implants and RTA at temperatures as close to the melting point as possible (e.g., 800-900°C). Under these conditions PL shows strong band-edge luminescence with evidence of activation of the implanted species, RS shows single crystal behavior also with evidence of activation, and RBS shows elimination of the surface damage peak. In addition, RBS shows that the initial damage peak must be kept less than $\approx$2000Å in order to achieve single-crystal regrowth. Both RS and RBS results suggest that polycrystalline material results if the initial amorphous region exceeds that critical thickness.

C. Electrical and profiling experiments are now in progress on a new ROME/RADC contract. We anticipate good electrical behavior under the conditions found to be optimum by the above techniques.

V. PERSONNEL

James L. Merz, Professor of Electrical and Computer Engineering -- Principal investigator.

Dimitry Kirillov, Postdoctoral Research Fellow, employed full-time on this contract from its inception until early 1984.

Gad Bahir, Postdoctoral Research Fellow, employed full-time on this contract from August 1984.

Raphael Kalish, Visiting Researcher from the Technion, Haifa, Israel, during the summer of 1984.

Arza Ron, Visiting Researcher from the Technion, Haifa, Israel, during the summer of 1984.

Steve Shatas, R&D Engineer for A. Gat and Associates, laser annealing with the Heatpulse system.

Thomas Sigmon, Professor of Electrical Engineering, Stanford University, assisted Bahir with the RBS experiments (at Stanford).

The contract also supported appropriate clerical and technical staff.

IV. REFERENCES

1. James L. Merz, Rome Air Development Center Interim Report RADC-TR-83-161, Air Force Systems Command, Griffiss Air Force Base, NY 13441, July 1983.

2. D. Kirillov and J. L. Merz, Energy Beam-Solid Interactions and Transient Thermal Processing, edited by J. C. C. Fan and N. M. Johnson, (Elsevier-North Holland, Inc., NY, 1984), Materials Research Society Symposia Proceedings, Boston, MA (Nov. 1983); p. 707-712.

3. D. Kirillov, J. L. Merz, R. Kalish and A. Ron, Appl. Phys. Lett., 44, 609-610 (15 March 1984).

4. D. Kirillov, J. L. Merz, R. Kalish and S. Shatas, J. Appl. Phys., 57, 531-536 (January 15, 1985).

5. D. Kirillov and J. L. Merz, Energy Beam-Solid Interactions and Transient Thermal Processing, edited by D. K. Biegelsen, G. A. Rozgonyi, and C. V. Shank (Elsevier-North Holland, Inc., NY, 1985), Materials Research Society Symposium Proceedings, Boston, MA (November 1984).

6. M. Mizuta and J. L. Merz, Appl. Phys. Lett., 43, 375-377 (15 Aug. 1983).

7. M. Mizuta and J. L. Merz, Japanese J. Appl. Phys., 23, 634-638 (May 1984).

8. M. Lax, J. Appl. Phys., 48, 3919 (1977).

9. M. Lax, Appl. Phys. Lett., 33, 786 (1978).

10. Y. I. Nissim, A. Lietoila, R. B. Gold and J. F. Gibbons, J. Appl. Phys., 51, 274 (1980).

11. D. Kirillov and J. L. Merz, J. Appl. Phys., 54, 4104-4109 (July 1983).

12. D. Kirillov, J. L. Merz, P. D. Dapkus, and J. J. Coleman, J. Appl. Phys., 55, 1105-1109, Feb. 15, 1984). Also, D. Kirillov and J. L. Merz, Proc. Soc. Photo-optical Instrumentation Engineers, Vol. 452, to be published.

13. D.K. Sadana, S.C. Shatas, and A. Gat, Microscopy of Semiconductor Materials, 1983, Inst. Phys. Conf. Ser. No. 67, p. 143, published by the Institute of Physics, London, England.

14. C. Pickering, P.R. Tapster, P.J. Dean, and D.J. Ashen, GaAs and Related Compounds, 1982, Inst. Phys. Conf. Ser. No. 65, p. 469, published by the Institute of Physics, London, England.

15. J.P. Lorenzo, D.E. Davis, K.J. Soda, T.G. Ryan, and P.J. McNally, Laser-Solid Interactions and Transient Thermal Processing of Materials, Ed. by J. Narayan, W.L. Brown, and R.A. Lenanas (North Holland, N.Y. 1983) p. 683.

16. A.N.M. Masum Choudhury, K. Tabatabaie-Alivi, and C.G. Fonstaf, Appl. Phys. Lett. 43, 381 (1983).

17. V.V. Negreskul, E.V. Russu, S.I. Radautsan, and A.G. Cheban, Sov. Phys. Semicond. 9, 587 (1975).

18. Jiang De-Sheng, Y. Makita, K. Ploog, and H.J. Queisser, J. Appl. Phys. 53, 999 (1982).

19. S. Bendapudi and D.N. Bose, Appl. Phys. Lett 42, 287 (1983).

20. G. E. Devlin, Y. L. Davis, L. Chase, and S. Geschwind, Appl. Phys. Lett., 19, 138 (1971).

21. C. S. Rama Rao, S. Sundaram, R. L. Schmidt, and J. Comas, J. Appl. Phys., 54, 1808 (1983).

22. P. H. Borchered, G. F. Alfvey, D. H. Saunderson, and A. D. B. Woods, J. Phys., C8, 2022 (1975).

23. A. Mooradian and G. Wright, Phys. Rev. Lett., 16, 999 (1966).

24. P. Auvray, A. Guivarch, H. L'Haridon, G. Pelous and M. Salvi, J. Appl. Phys., 53, 6202 (1982).

25. M. G. Grimaldi, B. M. Paine, M. A. Nicolet and D. K. Sadana, J. Appl. Phys., 52, 4038 (1981).

VII. APPENDIX: Earlier Work on CW Laser Annealing of InP.

cw laser-annealing behavior of Se^+-implanted InP investigated by ellipsometry

M. Mizuta[a] and J. L. Merz
Department of Electrical and Computer Engineering, University of California, Santa Barbara, California 93106

(Received 18 March 1983; accepted for publication 6 June 1983)

Damage removal of Se^+-implanted InP after cw Ar^+ laser annealing has been monitored by measurement of the optical extinction coefficient k. A gradual decrease in k as a function of laser power is observed for room-temperature ion-implanted InP samples, compared to a sharp decrease in k for ion-implanted Si. These data and electrical measurements indicate that the ion-implantation damage removal process for InP is more complex than for Si.

PACS numbers: 61.70.Tm, 81.40.Ef, 42.60. – v, 07.60.Fs

InP has attracted considerable interest recently because of its application to semiconductor lasers, microwave devices, and millimeter waves. For the latter devices, ion implantation plays a particularly important role in planar device processing of this material; a key problem, however, is the annealing of the implanted layer.

Lasers have been utilized to anneal the damage introduced by ion implantation in a variety of materials.[1] In comparison with the successful recrystallization of implanted Si using both cw[2,3] and pulsed-beam[4] annealing, only limited success has been reported for the case of III–V compound semiconductors, especially GaAs and InP (Ref. 5). Most of the successful annealing of implanted GaAs has been obtained with pulsed-beam techniques[6]; in this case, a higher degree of electrical activation has been obtained from samples implanted with a high dose of n-type impurities than for conventionally annealed samples. On the other hand, low-dose implants into GaAs have not been satisfactorily activated either by cw lasers[7] or pulsed beams.[8] Attempts to improve the annealing of low-dose implanted III–V compounds by increasing the laser power have resulted in unacceptable surface decomposition during the strong, highly localized heating, even for very short laser pulses. The difference between results obtained for high-dose and low-dose cases is not presently understood, and the optimum conditions for annealing low-dose implants have yet to be determined.

In this letter we present measurements of the extinction coefficient of Se^+-implanted InP following cw Ar^+ laser annealing. It is found that the extinction coefficient (k) determined by ellipsometry is a convenient yardstick in evaluating amorphism and/or randomness, even though a detailed analysis of the data is quite complicated, as previously reported for the case of Si (Ref. 9).

Semi-insulating (100) InP:Fe was used in this experiment. After samples were chemically mechanically polished

[a] Present address: Tokyo Institute of Technology, Imaging Science and Engineering Laboratory, Midori-ku, Yokohama 277, Japan.

 0003-6951/83/160375-03$01.00

with Br-methanol, Se^+ was implanted with an accelerating voltage of 160 keV into samples which were heated to 200 °C (HOT implant) or held at room temperature (RT implant).

The multiline output of a cw Ar^+ laser was used for annealing; the laser-scanning system was described previously,[10] and consists of a galvanometer mirror drive for scanning in one direction and a translation stage for sample motion in the perpendicular direction. The beam diameter was 100 μm, and each translation step after a galvanometer scan could be as small as 6 μm. The scanning speed used was typically 5 cm/s. Samples were cw laser annealed either at room temperature (temperature of the vacuum hold-down stage) or at elevated temperature (between RT and 400 °C).

The refractive index and the extinction coefficient of samples were determined from ellipsometer measurements, using a 5461-Å light source. Electrical activation was evaluated from measurements of the sheet resistivity and the Hall mobility of the samples which were processed photolithographically to produce standard Van der Pauw patterns.

We have observed no clear relationship between refractive index and scanned laser power, in contrast to results in Si which were reported previously.[11] We therefore restrict our interest to values of k, the extinction coefficient, as a function of laser power. As seen in Fig. 1, k is larger for RT-implanted samples than for bare (unimplanted) InP, indicating a disordered state of the implanted sample. This value is dependent on implant dose because of the different degree of amorphism produced by different doses. However, k reaches a constant value for doses exceeding a critical implant dose of 5×10^{13} cm^{-2}; this is consistent with results determined by changes in absorbed electron current[12] or Rutherford backscattering (RBS).[13] It seems that the extinction coefficient measurement is more sensitive than these other methods. A decrease in k is observed after annealing the RT-implanted sample for which the substrate was maintained at room temperature during anneal. With increasing laser power, k decreases monotonically towards the value observed for bare InP. However, this limit is never reached, since the power first approaches P_0, the laser power which produces thermal decomposition of the surface. P_0 was determined by optical microscope observation of the surface after a series of single laser scans; the laser power is increased for each scan until evaporation of phosphorus is observed. For the 5×10^{13} cm^{-2} dose in Fig. 1, the change in k takes place fairly sharply compared to the gradual change observed for the higher-dose case (5×10^{14}–5×10^{15} cm^{-2}). The reason for this is not clear at this time, but may be related to the fact that the lower dose may not produce a fully amorphous state. For comparison, we have measured the annealing power dependence of k for As^+-implanted Si. (Detailed experimental conditions are presented in Ref. 14.) A considerably sharper decrease of k can be seen for the case of cw laser-annealed Si, as shown in the inset of Fig. 1. In this case, complete electrical activation can be obtained[10] after the sharp, well-defined transition shown in the inset, which clearly corresponds to the amorphous-crystal transition.

The quite different behavior of k for InP compared with Si is believed due to a different recrystallization process; in fact, we have observed that the dependence of k on laser

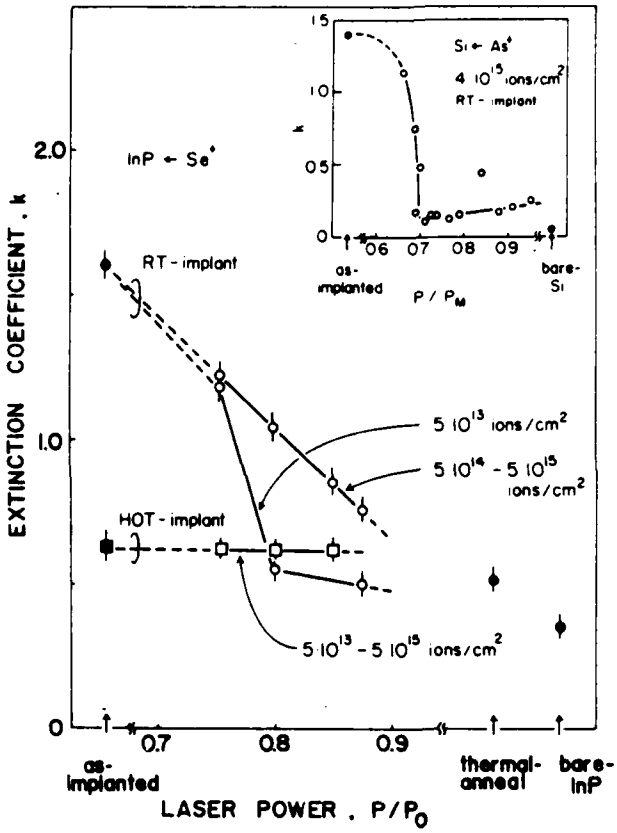

FIG. 1. Dependence of the extinction coefficient (k) of InP as a function of annealing laser power (P). P_0 is the power at which surface evaporation is observed using an optical microscope. Inset shows the extinction coefficient dependence upon laser power for Si. P_M represents the power at which the Si surface melts.

power for the case of GaAs is similar to that of InP. The only difference is that the critical dose was somewhat larger ($>10^{15}$ cm^{-2}) and not so well defined in the GaAs case. Apparently, this gradual decrease of k with laser power is typical of III–V compounds.

In the case of GaAs, the recrystallization process during furnace annealing has been reviewed.[15] At relatively low temperature (150–250 °C) an amorphized layer can grow epitaxially; however, a large density of crystal defects remains, which prohibits the electrical activation of implants and impurities (anneal stage I). An increase in anneal temperature (250–600 °C) gives rise to a reduction in the density of crystal defects, resulting in partial electrical activation (anneal stage II). A high degree of electrical activation with correspondingly high mobility cannot be obtained, however, unless the sample is heated to a sufficiently high temperature (600–900 °C) to anneal out the small defects and point defect complexes (anneal stage III). Ion-implanted Si, on the other hand, exhibits a single recrystallization stage, for which electrical activation and the removal of dense defects take place at the same time. Hence, as described before, a sharp decrease in k together with electrical activation is observed.

In our laser-annealed RT-implanted samples, shown in Fig. 1, no electrical activation was observed even after the reduction in k. According to the annealing behavior described above, this implies that, although the sample under-

went anneal stage I, a large density of crystal defects remains because the total laser power was insufficient to completely remove disorder. Either the total optical energy must be increased, or the degree of residual damage from anneal stage I decreased in order to obtain a higher degree of electrical activity.

Quite different results are observed for HOT implants, also shown in Fig. 1. In this case, the as-implanted sample shows a significantly lower value of k, and this value remains constant after laser annealing, indicating that the HOT-implant procedure can eliminate the annealing stage corresponding to the amorphous-crystalline transition (stage I). This result agrees with RBS measurements[15] in GaAs. Nevertheless, even for HOT implants, a large density of extended defects probably remains, because essentially no electrical activity is observed, except for a single case described below. It is noted that the value of k is still larger than the bare-InP case.

Among all the samples which were implanted HOT, only in one case was electrical activation observed, with sheet resistivity comparable to, and mobility somewhat lower than, thermally annealed samples which had a phosphosilicate glass cap during furnace anneal at 750 °C for 5 min. This case resulted when the samples were implanted with 5×10^{15} Se^+ cm^{-2}, and were laser annealed at elevated temperature; the substrate temperature (T_s) was held at 370–400 °C. From the blue appearance of the surface of these samples, we deduced that the surface was oxidized during the anneal. The oxide was found to develop nonuniformly, with a thicker oxide at the periphery of the sample, probably because the maximum temperature was attained at the edge of the sample. The mobility of the sample was rather low, 200–400 cm^2/Vs, while the sheet resistivity was reasonably good, 70–150 $\Omega/\square$. Although even lower values of T_s have been used, lower mobility and higher sheet resistivity (typically $\mu < 50$ cm^2/Vs and $\rho > 1000$ $\Omega/\square$ for $T_s = 250$ °C) resulted, as well as a reduction of surface flatness owing to an intermixing of the developing native oxide and the bare surface. A large number of samples implanted at doses between 5×10^{13} and 5×10^{15} cm^{-2} have been investigated in this work. Electrical activation is achieved, however, only for the highest dose samples. For lower doses, we believe that the implanted donor concentration was too low to overcome the density of compensating defect centers introduced by surface decomposition, as has been previously suggested by Davies *et al.*[16] Therefore, for the 5×10^{15} cm^{-2} sample described above ($T_s = 400$ °C), the implanted impurity concentration must be well in excess of the defect density; this results in reasonable electrical activation but low mobility.

From the results of these studies it is clear that, in order to achieve good electrical activation, higher power must be deposited in the sample to undergo the third stage of annealing; to reach such power without surface decomposition, a dielectric cap is necessary. In fact, the use of a phosphosilicate glass cap during anneal has yielded electrical activation with doses as low as 5×10^{12} cm^{-2}, which will be reported separately.

The authors would like to thank Don Zak for technical assistance, Dr. J. P. Donnelly and Dr. C. Kirkpatrick for implanting some of the samples, and Dr. D. E. Davies and Dr. J. P. Lorenzo for technical discussions and supplying additional InP substrates. This work was performed under Air Force contract F19628-79-C-0128, ROME/RADC, Hanscom AFB.

[1]Many examples are given in *Laser and Electron Beam Solid Interactions and Material Processing*, edited by J. F. Gibbons, L. D. Hess, and T. W. Sigmon (Elsevier, New York, 1981).
[2]A. Gat, J. F. Gibbons, V. R. Deline, P. Williams, and C. A. Evans, Jr., Appl. Phys. Lett. **32**, 726 (1978).
[3]J. S. Williams, W. L. Brown, H. J. Leamy, J. M. Poate, J. W. Rodgers, D. Rousseau, G. A. Rozgonyi, J. A. Shelnutt, and T. T. Sheng, Appl. Phys. Lett. **32**, 542 (1978).
[4]G. Foti, E. Rimini, W. S. Tseng, and J. W. Mayer, Appl. Phys. **15**, 365 (1978).
[5]F. H. Eisen, in *Laser and Electron Beam Processing of Materials*, edited by C. W. White and P. S. Peercy (Academic, New York, 1980), p. 309.
[6]S. G. Liu, C. P. Wu, and C. W. Magee, in *Laser and Electron Beam Processing of Materials*, edited by C. W. White and P. S. Peercy (Academic, New York, 1980), p. 341.
[7]C. L. Anderson, H. L. Dunlap, L. D. Hess, G. L. Olson, and K. V. Vaidyanathan, in *Laser and Electron Beam Processing of Materials*, edited by C. W. White and P. S. Peercy (Academic, New York, 1980), p. 334.
[8]M. H. Badawi, B. J. Sealy, K. G. Stephans, and J. A. Akintude, Jpn. J. Appl. Phys. **19**, Suppl. **19**-1, 139 (1980).
[9]T. Motooka and K. Watanabe, J. Appl. Phys. **51**, 4125 (1980).
[10]M. Mizuta, N. H. Sheng, and J. L. Merz, Appl. Phys. Lett. **38**, 453 (1981).
[11]K. Watanabe, M. Miyao, I. Takemoto, and N. Hashimato, Appl. Phys Lett. **34**, 518 (1979).
[12]W. Rothmund and C. R. Frizsche, J. Vac. Sci. Technol. **16**, 968 (1979).
[13]E. F. Kennedy, Appl. Phys. Lett. **38**, 375 (1981).
[14]M. Mizuta, N. H. Sheng, J. L. Merz, A. Lietoila, R. B. Gold, and J. F. Gibbons, Appl. Phys. Lett. **37**, 154 (1980).
[15]J. S. Williams and H. B. Harrison, in *Laser and Electron Beam Solid Interactions and Material Processing*, edited by J. F. Gibbons, L. D. Hess, and T. W. Sigmon (Elsevier, New York, 1981), p. 209.
[16]D. E. Davies, J. P. Lorenzo, and T. G. Ryan, Appl. Phys. Lett. **37**, 612 (1980).

JAPANESE JOURNAL OF APPLIED PHYSICS
VOL. 23, NO. 5, MAY, 1984 pp. 634-638

CW Laser Annealing of InP

M. MIZUTA* and J. L. MERZ

Department of Electrical and Computer Engineering, University of California, Santa Barbara, CA 93106, USA

(Received November 28, 1983; accepted for publication January 28, 1984)

CW Ar^+ laser annealing is used to activate semi-insulating InP after ion-implantation with Se. Electrical activation has been measured for a wide range of implant doses (3×10^{12} - 5×10^{15} cm^{-2}) using a phosphosilicate glass cap during laser annealing. The dependence of the resulting electrical properties on laser power and scan speed are investigated in terms of surface decomposition and slip line formation. Successive anodic oxidation coupled with Hall measurements has demonstrated that there is no impurity redistribution during CW laser annealing.

§1. Introduction

Recently, we have investigated the annealing behavior of Se-implanted, CW laser-annealed InP by ellipsometry.[1] Electrical activation, however, has not been obtained except at the highest dose (5×10^{15} cm^{-2}) because of apparent surface decomposition. Generally only a limited degree of success in obtaining electrical activation has been reported after laser annealing III-V compound semiconductors, especially GaAs and InP.[2-6] The main difficulty encountered in activating low-dose implanted III-V compounds is generally believed to result from surface decomposition during the strong, highly-localized heating, even for very short laser pulses. In a recent study of the pulse-annealing of bare (i.e., unimplanted) epitaxial GaAs,[7] the resulting mobilities were degraded for a considerable distance (~ 0.3 μm) below the surface of the sample; this distance corresponds to the typical projected range of implanted ions. Therefore, compensation of implanted donors may occur by the defects produced by surface evaporation, resulting in poor electrical activation even though the implanted impurities may end up in proper substitutional sites. This may indeed represent a crucial limitation for laser annealing, if the temperature required for complete activation is substantially higher than that associated with the onset of surface decomposition. These thermal effects may differ in degree for the various III-V compounds. Much less is known about the beam annealing of implanted InP than for GaAs.

In this paper we present results concerning the electrical activation of Se-implanted InP using CW Ar^+ laser annealing, both with and without the use of phosphosilicate glass (PSG) as a dielectric cap. Recrystallization occurs by solid-phase epitaxy, so that no melting of the surface occurs, avoiding significant impurity redistribution. The next section describes the experimental procedures used. Results and discussion are presented in §3, including measurements of the sheet resistivity (ρ) and the Hall mobility (μ). Slip line formation observed by optical microscopy, and the depth profiles of both ρ and μ are also discussed in this section. Finally, the results are summarized in §4.

§2. Experimental

Se^+ was implanted with an accelerating voltage of 160 keV into semi-insulating (100) InP:Fe samples which were heated to 200 C (HOT-implant) or held at room temperature (RT-implant). Phosphorus-doped SiO_2 (PSG), typically 1700 Å thick, was deposited onto some of the samples at 320-380 C in a silox reactor. The concentration of P in the PSG was chosen to be ~ 7-8%, so that the thermal expansion coefficient of the PSG was comparable to that of InP.[8] The composition of PSG was determined by electron microprobe analysis and Auger electron spectroscopy.[9] In some cases, Al metal was evaporated to cover the periphery of the sample; this was done to eliminate the temperature rise at the edge of the sample which usually occurs during annealing. In this way, very small samples could be uniformly annealed.

The multi-line output of a CW Ar^+ laser was used for annealing, together with the laser-scanning system described previously.[1,10,11] The laser spot was scanned with a speed between 0.5 and 50 cm/s. Electrical activation was evaluated from measurements of the sheet resistivity (ρ) of the samples which were processed photolithographically to produce standard van der Pauw mesa patterns.

Slip lines introduced by the laser scan were investigated using the Nomarsky differential interference (NDI) contrast mode of an optical microscope, either before or after processing by an electrochemical surface etching technique which will be described elsewhere. Finally, sample surfaces could be anodically stripped[12] in order to profile the electron carrier concentration and mobility.

§3. Results and Discussion

3.1 *Electrical activation, sheet resistivity and Hall mobility*

A large number of samples implanted at doses between 5×10^{13} and 5×10^{15} cm^{-2} have been investigated in this work; the results are summarized in Table I. Let us first consider those samples that are annealed without any sort of capping layer. It is clear that good electrical activation (as indicated by sheet resistivity values comparable to or lower than thermally-annealed samples) is achieved only for high-dose samples. For the lower dose, uncapped samples, we believe that the implanted donor concentration was too low to overcome the density of compensating defect centers introduced by surface decomposition, as has been previously suggested by Davies *et al.*[7] Therefore, for the 5×10^{15} cm^{-2} dose sample ($T_s \sim 400$ C), the implanted impurity concentration must be well in excess of the defect density; this results in reasonable

*Present address: Tokyo Institute of Technology, Yokohama 227

Table 1. Summary of electrical activation obtained for laser-annealed samples with different implant during laser anneal doses, both with and without a PSG cap. The substrate temperature (T_s) is indicated. Comparison is made with a thermally-annealed control-sample. Sheet resistivity ρ ($\Omega/\square$) and mobility μ (cm^2 Vs) are given by the upper and lower numbers, respectively, in each pair. The word NO signifies that these parameters were unmeasurable, while blanks represent the absence of an experiment.

DOSE (cm^{-2})	$T_{implant}$	LASER-ANNEALED			THERMALLY ANNEALED
		NO PSG CAP		PSG	
		T_s ~ RT	T_s ~ 400 C	T_s ~ 400 C	
3×10^{12}	RT				$\rho = 1080$
	HOT			3400 780	$\mu = 1900$
5×10^{13}	RT	NO		1800 60	100
	HOT		NO	120 1430	1550
1×10^{15}	RT	NO			25
	HOT			22 790	1040
5×10^{15}	RT	NO			18
	HOT	NO	75 400		910

electrical activation but low mobility.

From the results of our previous study[1] it is clear that, in order to achieve good electrical activation, higher power must be deposited in the sample in order to anneal out small defects and/or defect complexes; to reach such power without surface decomposition, a dielectric cap is necessary. There are several possible caps which could be used to prevent thermal decomposition. PSG is one choice, which has two obvious advantages: first, the film contains P, which effectively prevents the evaporation of the host atom, and secondly, the concentration of P in the film can be chosen to match the thermal expansion coefficient of InP. HOT-implanted samples with PSG which were annealed at $T_s = 380$–400 °C showed good electrical activation with reasonable mobility; for the case of the 5×10^{13} cm^{-2} dose sample, the best values obtained were $\rho = 120\ \Omega/\square$ and $\mu = 1430\ cm^2/Vs$ compared to values by the thermally amealed sample (750 °C, 15 min), $\rho = 100\ \Omega/\square$ and $\mu = 1550\ cm^2/Vs$, as shown in Table 1. These values were observed using samples of dimension $6 \times 6\ mm^2$, without any Al coating, using a laser-scanning velocity of 3 cm/s. The appearance of the oxide produced during annealing suggests that the annealing was often non-uniform, as mentioned above; the maximum temperature attained was therefore believed to be different between the edge and the center of the sample. To prevent this, Al was evaporated after deposition of the PSG and removed by photolithography and etching from all but the periphery of the sample; this simultaneously produced a van der Pauw pattern on the $3 \times 3\ mm^2$ sample. This procedure can be used to eliminate an undesirable temperature rise at the edge of the sample. In addition, this procedure eliminates the processing step usually needed to etch a mesa, because the implanted region underneath the Al-film is not electrically activated, and therefore has a sufficiently high resistivity to allow sheet resistivity measurements of the annealed portion above.

Using the sample configuration described above, the "annealing window" for successful annealing was determined by varying laser power and scan speed, while monitoring the sheet resistivity and the Hall mobility. The results are shown in Fig. 1 for three different values of scan velocity. Here, V is a normalized, dimensionless velocity which represents the ratio of the dwell time of the laser beam to the time required to reach the steady-state temperature condition: $V = va/2D$, where v is the velocity of the laser beam (cm/s), a is the radius of the beam spot (55 μm in this case) and D is the thermal diffusivity (0.066 cm^2/s) calculated from the known values of the thermal conductivity (0.13 W/cm-deg)[13] and specific heat C_p (1.99 Ws/cm^3deg)[14] at 800 °C. Apparently, as a result of using the PSG cap, higher power could be delivered to produce electrical activation for each value of V. As the laser power increases, the sheet resistivity decreases; however, the mobility reaches a peak and begins to decrease at still higher power. This decrease is believed to be due to the slip line formation described below.

In the range of dose studied here higher sheet carrier concentration, compared to that of the control sample, has been observed for high dose (5×10^{14} cm^{-2}) samples. This may result from the fact that CW laser annealing is capable of activating implanted impurities whose concentration exceeds the solid solubility. This is the case for the pulsed-

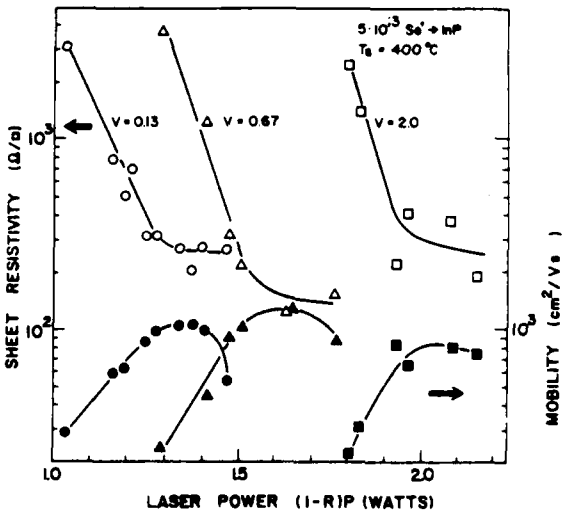

Fig. 1. Sheet resistivity (open points) and Hall mobility (solid points) of Se^+-implanted (5×10^{13} cm^{-2}, 160 kV) and laser-annealed InP with a PSG cap, plotted as a function of laser power with the different normalized scan velocities (V). $V = (a^2/D)(2a/v)$ where a is the radius of the beam (55 μm), D is the average thermal diffusivity (0.066 cm^2/s at 800 C), and v is the actual beam velocity (cm/s). The laser power is plotted after correcting for reflection loss from the PSG surface. Samples are $3 \times 3\ mm^2$, with a clover-leaf pattern surrounded by evaporated Al at the periphery of the sample.

beam annealing of GaAs[2, 6] or Si[20] and for the CW laser annealing of Si.[21] On the other hand, in the low-dose regime (3×10^{12} cm^{-2}), lower mobility has been observed than for the 5×10^{13} cm^{-2} dose sample. The reason for this behavior is simply not understood.

3.2 *Slip line formation*

From observations of the surface using an optical microscope, we found that these samples typically contain slip lines. The limitation of mobility is therefore believed to be due to the increase in slip line density. Similar results have been reported for GaAs,[15,16] for which slip lines are easily introduced during anneal due to a large thermal gradient. The formation of slip is probably not due to the stress between the PSG cap and the InP, because slip can develop even in a bare InP sample by using a high power laser scan. Figure 2 shows several examples of the development of slip lines, observed using NDI contrast microscopy. By comparing Fig. 2 with Fig. 1, it can be seen that slip lines develop at a fairly low power, for which the sheet resistivity has not yet reached a minimum value. As the power increases, the density of slip lines increases remarkably, as seen in Fig. 2(a) and (b). However, the decrease in mobility which occurs uppon further increase in laser power must be due to the creation of extended surface defects other than a higher density of slip lines, since no dramatic increase in slip line density is observed in Fig. 2(c). In the extreme high power case, cracks in the PSG cap, and the occasional intermixing of InP and PSG were observed; in this case the surface is no longer flat, resulting in severe degradation of the mobility. It has been reported[15] that the density of slip lines can be reduced if the velocity of the laser beam is slow enough to reduce the thermal gradient in the beam-scanning direction. However, we have obtained contradictiory results: a lower density of slip lines is observed in the sample scanned at higher beam velocity. This is seen in Fig. 3, where NDI photos are seen for three different scan velocities. The mobility values for the three samples are nearly the same, whereas V varies from 0.13 to 2.0, and lower slip density is observed for $V = 0.67$ and 2.0 than for $V = 0.13$. In fact we have achieved higher maximum mobility and lower sheet resistivity with

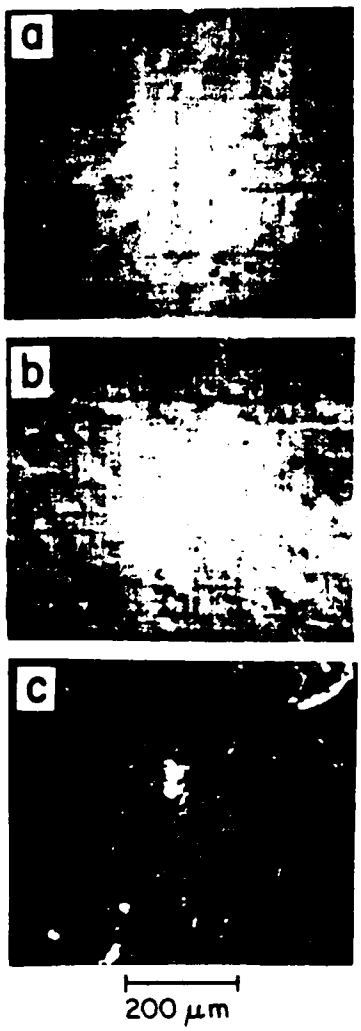

Fig. 2. Nomarsky differential interference (NDI) contrast optical micrographs for laser-annealed samples using a normalized beam-scan velocity (V) of 0.13, and different laser power. Annealing powers employed are (a) 1.19 W, (b) 1.34 W, and (c) 1.41 W.

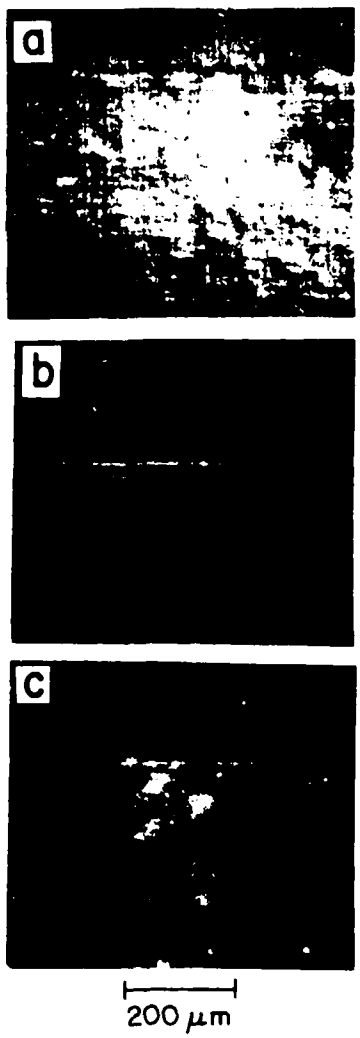

Fig. 3. NDI-contrast optical micrographs for samples annealed with different normalized scan velocity (V) and power. Annealing laser power and scanning velocity are (a) 1.34 W and $V = 0.13$, (b) 1.51 W and $V = 0.67$, and (c) 2.08 W and $V = 2.0$.

$V=0.67$ compared to the values with $V=0.13$. Further increases in V from 0.67 to 2.0, however, result in lower maximum mobility, probably because the dwell time was insufficient to anneal out the defects. This is not surprising for the case $V=2.0$.

The influence of slip on the electrical properties of InP seems somewhat different from the GaAs case, reported by Fan *et al.*[15] In their investigations, slip lines were introduced at high scan speeds by increasing the laser power; the sheet carrier concentration was observed to decrease with laser power, until anistropy was observed in the van der Pauw measurements. On the other hand, in the InP results reported here, the sheet carrier concentration always increases monotonically with laser power until heavy deterioration of the surface is observed. The mobility also increases, despite the fact that a large increase in the density of slip lines is observed (Fig. 2(a) and (b)). No anisotropy was observed in the measurement of the sheet resistivity, except that etching proceeds very rapidly along the slip lines during the photolithographic process used to make the mesa. The differences of the dependence of the electrical properties on slip between InP and GaAs might be due to differences in the electrical activity of dislocations in these materials; for InP, surface states may not produce energy levels in the forbidden gap, so that non-ionized dislocations do not act as severe scattering centers. Nevertheless, slip lines are undesirable, even if they do not act as mobility killers, because they tend to limit the maximum mobility attainable, and increase surface roughness, a potentially serious problem for device processing. Possible ways to eliminate the formation of slip include (a) increasing the substrate temperature (T_s) to reduce the thermal gradient, and (b) increasing the scan speed in order to shorten the dwell time. The latter case is in fact realized in the case of annelaing implanted Si with nsec pulsed laser beams, for which very rapid cooling of the crystal takes place, and no dislocation formation results.[17] In other words, the velocity of dislocation motion is so low compared to the cooling time, that the large strain which would develop slip is frozen in the crystal. There is little reliable data concerning dislocation motion in InP; we there fore used the velocity of dislocation in Si.[18] The actual beam velocity, $v=48$ cm/s (corresponding to $V=2.0$) is comparable to or faster than the velocity of dislocation motion in Si (10 cm/s). The reduction in the density of slip lines with increasing scan velocity, shown in Fig. 3, can be explained in this way. However, from the point of view of defect annealing, this dwell time is so short that a higher temperature is required for the complete removal of lattice defects.

The temperature due to laser heating was estimated using the approach of Lax;[19] the maximum temperature estimated in this way was 670 C at $(1-R)P=1$ watt and 850 C at 1.5 watts with $T_s=400$ C and $a=55$ μm, assuming that the beam is stationary ($V=0$; cf. Fig. 4). For the actual moving beam, the maximum temperature rise was estimated to be 650–800 C within the laser power range of 1–1.5 watts when $V=0.13$, and 690–780 C at 1.8–2.15 watts when $V=2.0$. Temperatures for the non-stationary beam case were determined by shifting the curve obtained for the stationary case. A multiplying factor was used which is the ratio between values of P_0 for which the

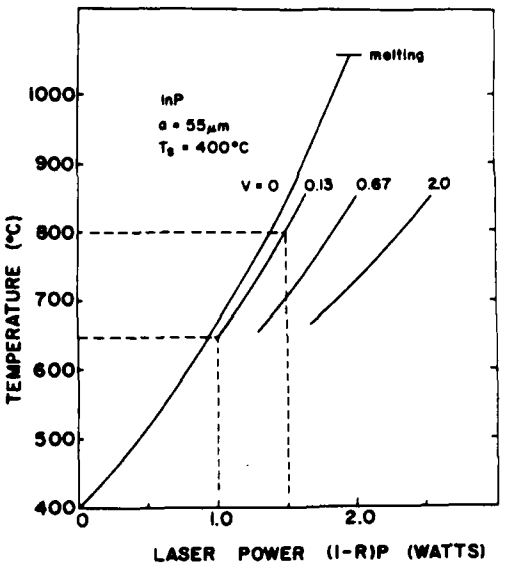

Fig. 4. The temperature rise induced by the laser local heating. For the stationary beam case ($V=0$), the temperature is calculated including the effect of nonlinear thermal conductivity on temperature, with a substrate temperature T_s of 400 C. For the moving beam case, the curve is simply shifted by a factor which is determined experimentally (see text).

surface evaporation pattern appears identical for each different value of V. However, regardless of the scan velocity, cracks and/or heavy surface deterioration were observed, as described previously, at substrate temperatures approaching 800 C. Therefore, simply decreasing the dwell time and increasing the laser power may not be a suitable way to optimize annealing.

3.3 *Depth profiles of the carrier concentration and mobility*

Stripping of the layer by anodic oxidation and etching was used to profile the electron carrier concentration and the Hall mobility.[12] The result for a laser-annealed sample, as shown in Fig. 5, indicated little or no redistribution of

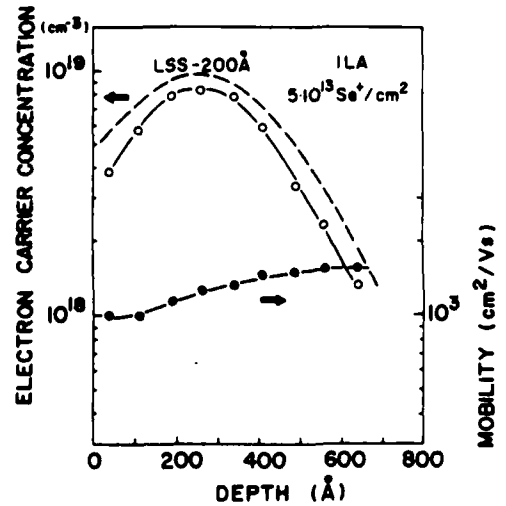

Fig. 5. Depth profiles of electronic carrier concentration (open circles) and Hall mobility (solid circles). The broken line represents a calculated LSS range profile, but shifted by 200 A towards the surface to include the effect of PSG-InP inter-mixing.

the implanted species; this result was expected for CW laser annealing. However it was found that the range of the profile was significantly displaced from the calculated LSS profile. This can be explained by the expected mixing of PSG and InP over a distance of 200 Å; a similar effect has been reported in the case of SiO_2 on InP.[22] The LSS curve drawn in the figure was shifted by 200 Å towards the surface, and agrees well with the measured carrier profile. This indicates that ~200 Å of InP was removed during etching of the PSG cap. This intermixing of PSG and InP was also observed for the control sample, which was furnace-annealed in flowing N_2/H_2 at 750°C for 15 min.

Comparison of the concentration and mobility profiles of samples annealed at different laser power shows that there are differences in the mobility profiles, whereas concentration profiles are quite similar, differing only in absolute value. For samples annealed at low power, the mobility is lower at the surface; on the other hand, the mobility is lower below the surface for samples annealed at higher power. In all cases, however, the measured values of mobility are still lower than the values calculated from the carrier concentration measurements. These results suggest that laser-induced-damage and/or slip formation governs the mobility. In the case of the control sample, the mobility is lower in regions where the carrier concentration is high, indicating that the mobility is limited by ionized scattering, rather than by slip-line formation. In fact, slip lines were not observed in the control sample. However, this sample showed a slightly broadened carrier profile due to the diffusion of implanted Se, as expected for furnace annealing.

It is also interesting to investigate the effect of Al masking, used to avoid excess heating at the edge of the sample, on mobility. Surprisingly, we found that improved values for ρ and μ are obtained without the Al mask (values shown in Table 1 for a dose of 5×10^{13} cm^{-2}) compared to the values obtained when Al masking is used (data shown in Fig. 1). This fact may be understood by assuming that the absence of the Al mask allows the overall substrate temperature to increase somewhat, so that less slip formation occurs, and the annealing mechanism is closer to that of the furnace anneal.

§4. Conclusion

InP implanted with Se^+ was successfully annealed by a CW Ar^+ ion laser utilizing phosphosilicate glass as a dielectric cap. A wide range of Se^+ dose was activated for hot implants when the substrate was heated to 400°C during laser anneal. For low-dose implants, μ was somewhat lower than was obtained in thermally-annealed control samples. For medium doses, ρ and μ become comparable to the controls, whereas in the high-dose cases, ρ can be lower than the thermal-anneal values. The best results obtained in this work, which were comparable to furnace-annealed control samples, were observed for a HOT-implant dose of 5×10^{13} cm^{-2}, and laser annealing through a PSG cap with $T_s = 400$°C. In every case no impurity redistribution was found in laser-annealed specimens. The formation of slip lines, which can be reduced but not eliminated by rapid scanning, is found to have a serious negative effect on the electrical properties of laser-annealed InP.

Acknowledgement

The authors would like to thank Don Zak for technical assistance, J. P. Donnelly and C. Kirkpatrick for implanting some of the samples, and D. E. Davies and J. P. Lorenzo for technical discussions and for supplying additional InP substrates. This work was performed under Air Force Contract F19628-79-C-0128, ROME/RADC, Hanscom AFB.

References

1) M. Mizuta and J. L. Merz: Appl. Phys. Lett. **43** (1983) 375.
2) F. H. Eisen: *Laser and Electron-Beam Processing of Materials*, eds. C. W. White and P. S. Peercy (Academic Press, New York, 1980) p. 309.
3) S. G. Liu, C. P. Wu and C. W. Magee: *Laser and Electron-Beam Processing of Materials*, eds. C. W. White and P. S. Peercy (Academic Press, New York, 1980) p. 341.
4) C. L. Anderson, H. L. Dunlap, L. D. Hess, G. L. Olson and K. V. Vaidyanathan: *Laser and Electron-Beam Processing of Materials*, eds. C. W. White and P. S. Peercy (Academic Press, New York, 1980) p. 334.
5) M. H. Badawi, B. J. Sealy, K. G. Stephans and J. A. Akintude: *Proc. 11th Conf. (1979 Int.) Solid State Devices Tokyo, 1979*, J. Appl. Phys. **19** (1980) Suppl. **19-1**, p. 139.
6) N. J. Shah, H. Ahmad, J. R. Sanders and J. F. Singleton: Electron. Lett. **16** (1980) 433.
7) D. E. Davides, J. P. Lorenzo and T. G. Ryan: Appl. Phys. Lett. 37 (1980) 612.
8) J. P. Donnelly and C. E. Hurwitz: Appl. Phys. Lett. **31** (1977) 418.
9) G. Queirolo and G. U. Pignatel: J. Electrochem. Soc. **127** (1980) 2438.
10) M. Mizuta, N. H. Sheng and J. L. Merz: Appl. Phys. Lett. **38** (1981) 453.
11) M. Mizuta, N. H. Sheng, J. L. Merz, A. Lietoila, R. B. Gold and J. F. Gibbons: Appl. Phys. Lett. **37** (1980) 154.
12) J. P. Lorenzo, D. E. Davies and T. G. Ryan: J. Electrochem. Soc. **126** (1979) 118.
13) I. Kudman and E. F. Steigmeiner: Phys. Rev. **133A** (1964) 1665.
14) M. Boutard and P. Pinard: J. Phys. 33 (1972) 787.
15) J. C. C. Fan, J. P. Donnelly, C. O. Bozler and R. L. Chapman: *Proc. 7th Int. Symp. on GaAs and Related Compounds, St Louis, 1978* (Institute of Physics, London, 1979) p. 472.
16) C. L. Anderson, H. L. Dunlap, L. D. Hess and K. V. Vaidyanathan: *Laser-Solid Interactions and Laser Processing*, eds. S. D. Ferris, H. J. Leamy and J. M. Poate (AIP, New York, 1979) p. 585.
17) J. Narayan, R. T. Young and C. W. White: J. Appl. Phys. **49** (1978) 3912.
18) V. N. Erofeev, V. I. Nikitenko and V. B. Osvenski: Phys. Status Solidi **35** (1969) 79.
19) M. Lax: Appl. Phys. Lett. 33 (1978) 786.
20) C. W. White, S. R. Wilson, B. R. Appleton and R. T. Young: J. Appl. Phys. **51** (1980) 738.
21) A. Lietoila, J. F. Gibbons, T. J. Magee, J. Perg and J. D. Hong: Appl. Phys. Lett. **35** (1979) 532.
22) T. Nishioka and Y. Ohmachi: J. Appl. Phys. **51** (1980) 5789.

MISSION
of
Rome Air Development Center

RADC plans and executes research, development, test and selected acquisition programs in support of Command, Control Communications and Intelligence (C^3I) activities. Technical and engineering support within areas of technical competence is provided to ESD Program Offices (POs) and other ESD elements. The principal technical mission areas are communications, electromagnetic guidance and control, surveillance of ground and aerospace objects, intelligence data collection and handling, information system technology, solid state sciences, electromagnetics and electronic reliability, maintainability and compatibility.

Printed by
United States Air Force
Hanscom AFB, Mass. 01731

END

12-86

DTIC